ADDIS ABABA UNIVERSITY

SCHOOL OF GRADUATE STUDIES

SCHOOL OF EARTH SCIENCE

GEOLOGY, GEOCHEMISTRY & GENESIS OF GOLD MINERALIZATION IN ASHASHIRE PROSPECT, BENISHANGUL-GUMZ REGION, WESTERN ETHIOPIA

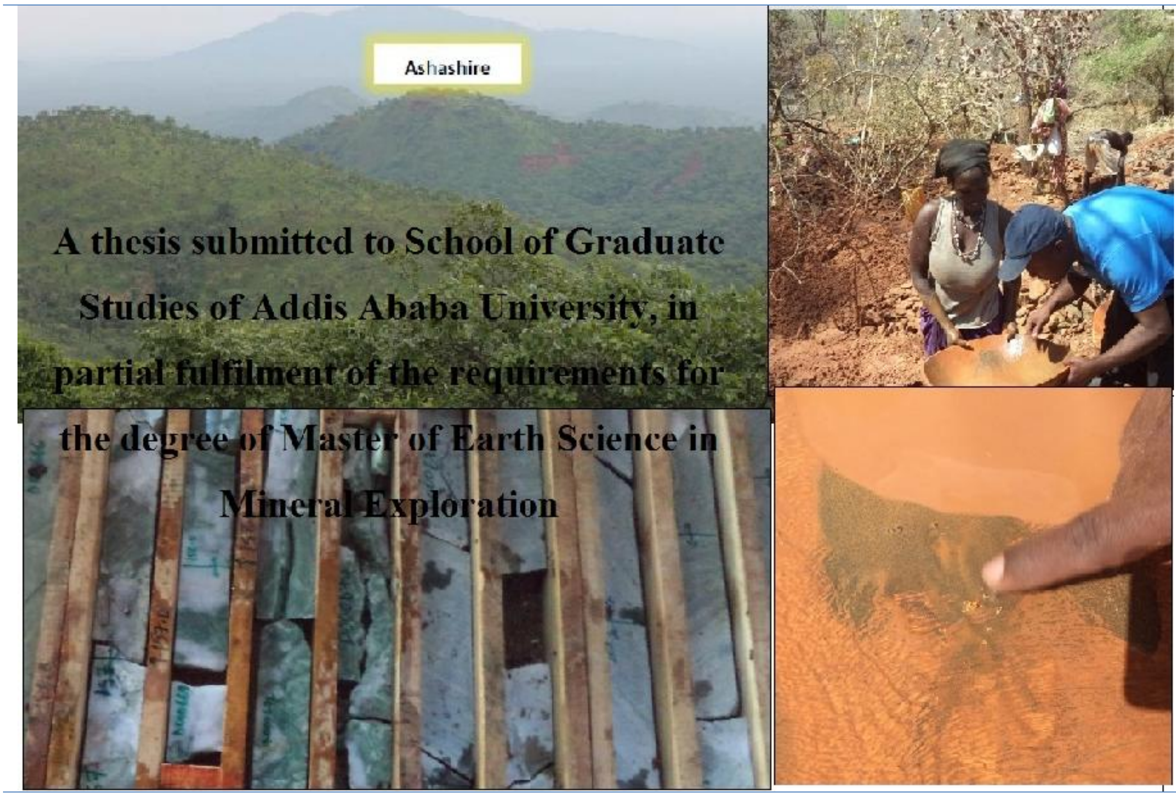

BY: ABEBE BEDASSA
5/30/2014

ADDIS ABABA UNIVERSITY

COLLEGE OF NATURAL AND COMPUTATIONAL SCINCES

SCHOOL OF GRADUATE STUDIES

SCHOOL OF EARTH SCIENCES

GEOLOGY, GEOCHEMISTRY & GENESIS OF GOLD MINERALIZATION IN ASHASHIRE PROSPECT, BENISHANGUL-GUMZ REGION, WESTERN ETHIOPIAN

A THESIS SUBMITTED TO SCHOOL OF GRADUATE STUDIES OF ADDIS ABABA UNIVERSITY, IN PARTIAL FULFILMET OF THE REQUIREMENTS FOR THE DEGREE OF MASTER OF EARTH SCIENCE IN MINERAL EXPLORATION

ABEBE BEDASSA

30/05/06

ADVISOR: PROF. SOLOMON TADESSE

CO-ADVISOR: AYELE KEBEDE

ADDIS ABABA UNIVERSITY

COLLEGE OF NATURAL AND COMPUTATIONAL SCINCES

SCHOOL OF GRADUATE STUDIES

SCHOOL OF EARTH SCIENCES

GEOLOGY, GEOCHEMISTRY & GENESIS OF GOLD MINERALIZATION IN ASHASHIRE PROSPECT, BENISHANGUL-GUMZ REGION, WESTERN ETHIOPIAN

BY:ABEBE BEDASSA

APPROVED BY EXAMINING BOARD **SIGNATURE**

Chairman

Dr. Tesfaye Kidane ______________

Advisor

Prof. Solomon Tadesse _______________

Co-Advisor

Ayele Kebede (M.Sc.) _______________

Examiners

Dr.Werash Getaneh _______________

Dr.Mulugeta Alene _______________

ACKNOWLEDGMENT

I would like to thank very much Professor Solomon Tadesse for his decisive guidance, follow-up, support, constructive comments and suggestions. I am also grateful to him for providing valuable reference material and sharing his field and research experience throughout this thesis work.

I am very grateful to Ayele Kebede, country manager at Benzu-Gold Fields Ltd Gold Exploration Company, for permitting me to work in Ashashire project, for giving me technical and accommodations support. I also appreciate his follow-up, comments and encouragement from the beginning to the end of my study.

A lot of thanks go to Tesfaye Regassa and Geremu Fufa for their incredible help during the laboratory work and consistent suggestion over the whole work.

I would like to thank very much the Norwegian government for allowing me to cover living expense, school fee and full access to laboratory expenses after my return from Norway.

DECLARATION OF ORIGINALITY

This thesis is my original work and has not been presented for a degree in any other university, and that all sources of material used for the thesis have been duly acknowledged.

Abebe Bedassa.

TABLE OF CONTENT

LIST OF FIGURES

LIST OF TABLES

ABSTRACT

The study area, Ashashire prospect, is located, in Benishangul-Gumz region western Ethiopia, about 741 km west of Addis Ababa.

Field observation and petrographic study shows that the prospect comprises various units that include granite, plagioclase-muscovite (sericite)-quartz schist, quartz vein, actinolite-quartz-chlorite schist, carbonitized chlorite-sericite-quartz schist and metasediments. Based on the critical mineral assemblages, the majority of the units are metamorphosed to green schist facies. Field observation and thin section analysis also revealed that the study area experienced at least three phase of deformations that are manifested by various structures.

Fourteen samples are analyzed for major and trace elements using XRF method. Among the variation diagrams, only the graphs of K_2O vs. Al_2O_3 and K_2O vs. CaO show positive correlation. On the other hand, K_2O is negatively correlated with MgO, Na_2O and SiO_2. Chondrite normalized (wood et al.1979b) spider diagram shows the pattern of the trace elements, particularly the pattern of high field strength elements (HFSE) Zr, Ti & Y, are generally similar, that implies the rocks are genetically related i.e. they have similar source rock. The discrimination diagram (Ti vs. Zr) shows the majority of the rocks of Ashashire area have similar tectonic environment as rocks formed in island arc tholeiites, calc-alkali basalt and mid oceanic ridge basalt (MORB) zone.

Statistical analysis of AAS results of gold from forty samples showed a range of gold concentration from < 0.02-48.5 ppm and mean value of 2.88ppm. The histogram indicates about 49 percent of the samples have shown anomalous Au value i.e greater than 0.5ppm. Correlation value and the scatter diagrams of Au with the multi elements (Ag, Cu, Pb, Zn, Ni, Co and Mn) showed that gold has stronger positive association with silver (Ag) only.

Based on field observation and textural relationship of ore minerals the gangue minerals that constitute the host rock are formed in the earliest phase and followed by magnetite hematite, ilmenite, pyrite; chalcopyrite and gold are crystallized respectively.

The geological and structural setting, host rock alteration and gangue mineralogy are suggestive for a shear-zone hosted orogenic-gold type deposit at Ashashire.

CHAPTER ONE

1 INTRODUCTION

1.1 Back ground

Ashashire prospect area is geologically situated in western Green Stone Belt (WEGSB), of Precambrian rocks of Ethiopia which are a constituent of the East African Orogen (EAO). The East African Orogen (EAO) is a belt of deformed metamorphic rocks which comprises two major segments: the Arabian–Nubian Shield (ANS) in the north, and the Mozambique Belt in the south (Stern 1994; Stern, 2002) (Figure 1.1). The orogen covers a large area stretching from Mozambique in the south, to the Arabian Peninsula in the north and it was formed during the collision of East and West Gondwana in the Neoproterozoic (Johnson et al., 2003).

The Precambrian terrain of Western Ethiopia consists of the two major lithotectonic blocks, that is high-grade gneissic–migmatitic associations (Mozambique Belt) and low-grade metavolcano-sedimentary sequences (ANS), unlike the other part of the basement exposure of the country that comprise either Mozambique Belt or Arabian–Nubian Shield (ANS) Figure. 2.3. It is also intruded by syn- to late-tectonic granodioritic and granitic plutons (Asrat et al.2001).

Generally the Precambrian rocks of Western Ethiopia are grouped into five major domain (Alemu and Abebe, 2000; Tadesse and Allen, 2005) (Figure 2.4). These are: granitoids, Sirkole volcano-sedimentry sequences, Dengi volcano-sedimentry-plutonic sequences, Tulu Dimitu-Barudu volcano- sedimentry sequences and gneisses and migmatites. Among the domains, it is a sirkole volcano-sedimentary sequence, which is part of ANS, comprises the Ashashire prospect. The ANS has been the source of gold since Pharaonic Egypt. Nowadays the Sheld has become the major target for mining and mineral exploration activity, particularly in Sudan, Arabia, Eritrea, and Ethiopia (Kroner and Stern, 2005). Consequently the Ashashire prospect has been the target of gold exploration for over two decades as the other prospective targets in the ANS parts of Ethiopia.

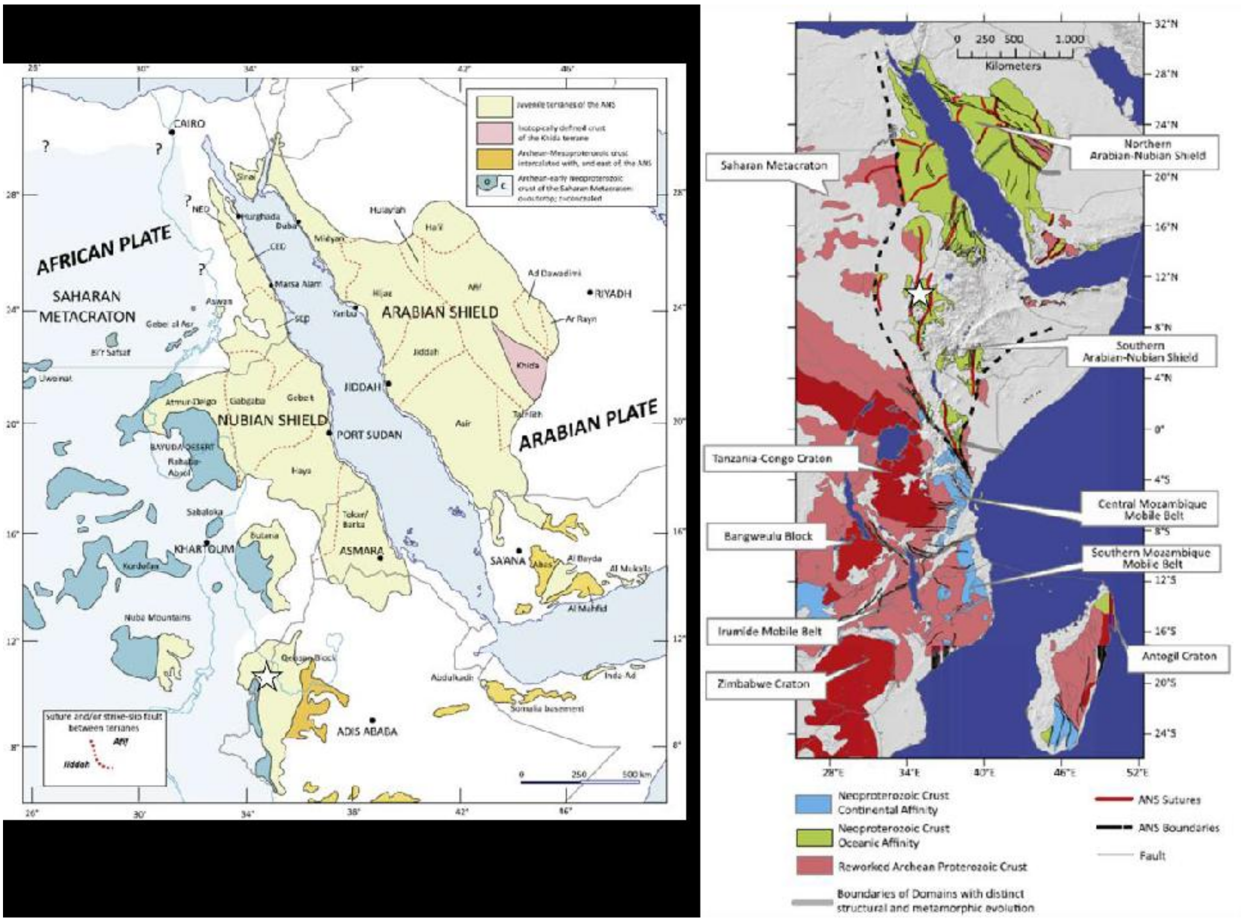

Figure 1.1 Arabian-Nubian shield (L) and regional tectonic framework (R) showing location of the study area in the white star on each image (from Johnson et al., 2011).

1.2 Statement of the problem

Western Ethiopia covers the largest green stone belt of the country that consists of various Precambrian rocks. The belt is known for hosting different types of mineralization that are associated to different lithologies and styles of mineralization (Golden Star Resources, 1996). Ashashire prospect is one of these areas in the belt where advanced gold exploration has lately been carried out by joint work of Gold Fields Ltd and Benzu Gold Mining Ethiopia PLC for the last three years. The companies, like most exploration companies, focus on grade and tonnage rather than studying the chemistry of associated base metals, petrology and genesis of the ore minerals. As a result, very few academic works has been done so far in the region. This research work may contribute in understanding the occurrence, geochemical relation of gold and base metals mineralization, and the genesis of gold mineralization at Ashashire and adjacent prospects.

1.3 Geography of the study area

The Ashashire prospect is located in Benishangul-Gumz region, western Ethiopia about 741 km west of Addis Ababa and 15 km east of the Ethio-Sudan border town of Kurmuk. The study area lie in geographical UTM coordinates system of 1165800N-1167200N and 654800E- 655600E (Figure1.1). It can be accessed either by an asphalted road from Addis Ababa through Asosa-Komosha-Kurmuk road or by flying from Addis to Asosa.

The climate of the study area is tropical with long dry season from December to May, and a rainy period from June to September, sometimes continuing in to October. The temperature ranges between 25^0c and 35^0c and sometimes above 40^0c commonly in April.

The physiography is characterized by rugged topography, parallel ridges and elevated area varies from 970 m to 750 m above sea level. Low lands dominate in the west portion, while the eastern part forms hills and mountain ridges. Most of the streams flow westwards and they are intermittent. The stream that flows E-W, crosses the northern part of the project area is a tributary of kota worke in which artisanal miners are active. Vegetation is sparse and some of the vegetation in the area consisting elephant grass, thorny bushes, acacia, incense trees and bamboo, reflecting the arid and semi-arid climate in the region. Thick tree growth is mainly confined to river valleys.

The area is populated by indigenous Benishangul people of Berta tribes living in groups in scattered villages, normally near streams. They are generally bilingual, speaking Arabic and Berta languages and followers of Muslim religion. The inhabitants are engaged by artisanal method gold panning in the valleys and little agricultural activities. Nowadays, mechanized farming activities are practiced by investors in areas between Asosa and Sirkole. Wild life habitat in the area includes several varieties of antelope, monkey, lion and others. Because of the tropical type of climate, weathering activity is so intense and thick soil formation is evidenced along the section of streams and weathering mantle section of the drill holes.

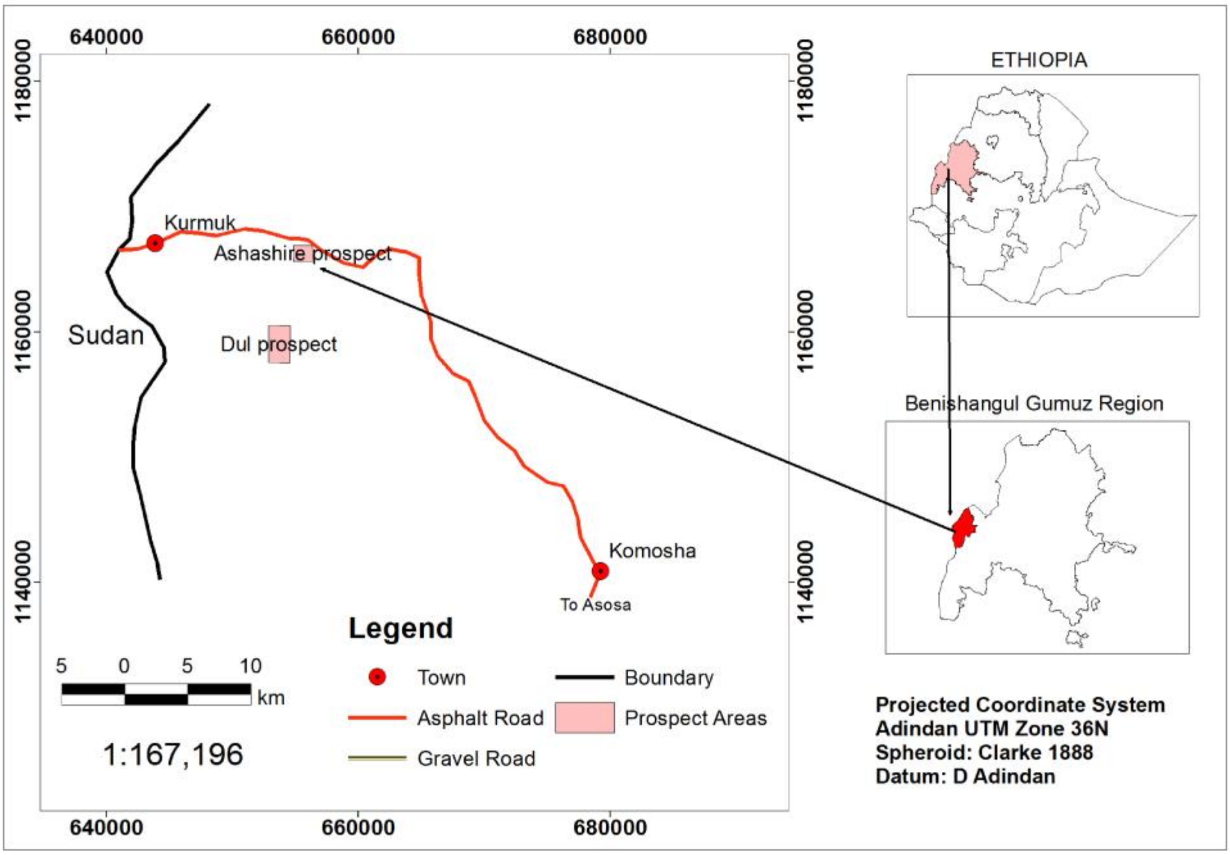

Figure 1.2 Location Map of the study area.

1.4 Objectives

1.4.1 General Objective

The research objective is to understand the gold mineralization at Ashashire prospect.

1.4.2 Specific Objectives

- To identify the nature and type of host rock, structure and other factors that control mineralization.
- To understand the gold geochemistry of the area.
- To understand the mineral paragenesis, their sequence and associated elements.
- To outline the extent of gold mineralization and propose genesis of gold on field and laboratory data.

1.5 Research Methodology

1.5.1 Field work

Various tasks have been accomplished before starting the field work. The office work includes review literatures, scientific journals and relevant books. Previous exploration work of Geological Survey of Ethiopia and Golden Star Resources (GSR) were reviewed; including assay results from stream sediment, soil, and trench channel samples. The previous geological map (1:25,000) made by GSR is used as a base map and modified and enlarged to produce 1:10,000 large scale map. Geological mapping and structural data have been done by systematically selecting four east-west traverse lines so as to cross the general N-S trending regional structures/ dominant foliation and to find maximum lithological and structural variations. The outcrops are described in terms of color, mineralogy/composition, texture/fabric and structures (foliation, lineation, fold, joints, veins), gross characteristics (fracture, weathering, ridge-former); and also the type of contacts between the units are attempted to describe. Besides, during the geological mapping the location of the drill holes have also been measured by Garmin GPS.

In addition to mapping five days were spent to log drill cores and collect samples from selected five drill holes. Among the five drill holes two of them were drilled using reverse circulation drilling (RC) method and the associated bulk duplicate samples have been taken.

Then the whole representative samples that have been collected from outcrops and drill hole are labeled and carefully inserted in separate plastic bags i.e. one bag for one sample in order to avoid contaminations. Furthermore, during mapping, core logging and sampling, several photos have been taken, using a Sony digital camera with 16mega pixels, so as to make the descriptions more clear.

1.5.2 Laboratory data analysis

1.5.2.1 Petrography /thin section preparation and description

Twelve thin sections have been prepared at geological survey laboratory from selected outcrops and cores at the central laboratory of GSE and the following procedure is followed;

- Cutting core sample approximately to a thickness of 5 millimeter at the required orientation.
- Trimming to prepare a rectangular slab of 50 mm *25 mm* 5 mm.

- Grinding one face of the slab by diamond impregnated rotary grinding wheel and using silicium carbide (SiC) grinding powder grade-400. The final grinding was performed by the same grinding powder-1000 using a different rotary grinding wheel to produce smooth and even surface.
- Mounting of the smoothed surface of the slab on glass slide using a different a resin formed by mixing Arladi AY-100 and Harter HY-951 at the ratio of 10:1 respectively.
- Drying of sample in a dryer at the temperature of $40^{o}C$ for 48 hours.
- Re-sectioning of slab to a thickness of approximately 1mm using low speed grinding wheel.
- Further **hand grinding** using Si-C grinding powder grade-600 on a glass plate. The final grinding was performed by the same grinding powder but grade-1000 to produce a thickness of 5 micron meter.
- Covering of the thin section with fluid spray of carbon compound and drying in an oven at a temperature of $40^{o}C$ for 30 minutes.

Thin sections have been examined under Leica petrography microscope for identification of transparent minerals such as silicates and calcite. It is also used to describe the texture and /or micro structures of the samples and to name the rock.

1.5.2.2 Polished section preparation and description

Fourteen samples for polished section/ore microscopy have been selected from altered and mineralized zone of core section. Preparation of polished sections has been done at Ethiopian geological survey laboratory. The preparation procedure is similar to that of petrographic thin section in most steps. In polished section the final polishing is done by mounting the sample on a rotary machine and the polishing process continued to produce an even and smooth surface of sample with wide of 30 micrometer. At this stage the sample is ready to be investigated by ore microscopy to determine mineral composition, ore mineral texture, alteration type, to determine ore and gangue minerals and their paragenetic sequence. The ore microscopic is conducted using German made Leica model.

B) Atomic Absorption Spectrophotometry (AAS) for gold and basemetals

RC drilling bulk duplicate samples and chip core samples are analyzed for wet assay using AAS at Ezana Analytical Laboratory in Mekele, Ethiopia; to know elemental concentration of gold and base metals.

The laboratory has used the following procedures to prepare the samples.

- Samples are dried, crushed to 2mm size, splitted 200g and pulverized to 75µm.
- Analysis is performed with Varian Atomic Absorption Spectrophotometer (AAS), Spectra AA240FS.
- During analysis accredited method is applied, to get a more precise result, which uses Aqua Regia digest with a method code AA74D2.The detection limit for gold is 0.02 ppm, for Ag is 0.2 ppm but for the rest of base metals is 1 ppm.

Table 1.1 To show the methods of sample preparation and analysis (Source: Ezana Laboratory Brochure, Mekele, Ethiopia).

Method Code	Description
PG210	Dry, crush to 2mm, split 200g, pulverize to 75 micrometer
AA74D2	50 g Aqua Regia digest-AAS finish, 0.02 ppm, gold
AA74D2	Aqua Regia digest-AAs finish, subsequent (Ag, Cu, Co, Pb, Ni, Zn, Mn)

C) X-Ray Fluorescence (XRF)

XRF is the most widely used analytical technique in determination of the major oxides such as ($Si0_2$, Al_2O_3, Fe_2O_3, CaO, MgO, Na_2O, K_2O, Tio_2, MnO, P_2O_5) and trace elements including Sr, Sc, Y, Ba, Zr, Nb, Mo, Pb, Zn, Co, and Cu. Samples for XRF are analyzed at central laboratory of Geological Survey of Ethiopia. Core samples and pulp from the remaining of AAS analysis are used in determination of the major and trace element chemistry of the rock.

Philips X-ray fluorescence spectroscopy model PW 2400 was used to analyze major, minor and trace elements in the pellets. The rock samples are crushed using aluminum jaw crusher and pulverized by agate disc grinder to -200 mesh consequently fused and pressed pellets are prepare and excited with x-ray radiation, that normally generated by an x-ray tube operated at a potential between 10 and 100 kilo volt.

The reason why fused pellets are prepared mainly for major elements and pressed pellets for minor and trace elements is that in preparation of the pressed pellets the amounts of foreign substances has to be low so that the concentration of trace elements will not get further diluted; and the analysis does not show below detection limit, but during the preparation of fused pellets there are different admixture to the sample. Since it is a major element analysis expressed in percent, it will not affect concentration of the element so much. Detection limits for many of these trace elements lie in the range of 1-10 ppm, under routine operating conditions. Every sample is analyzed utilizing the whole rock analysis. This measured the major elements present in each sample (Si, Al, Ca, Mg, Fe, Mn, Na, K, P, Ti) and trace elements.

1.5.3 Geological and geochemical data analysis

Geological and geochemical data are analyzed using different software such as Arc GIS 10, Petrograph 2beta and IBM SPSS statistics software version 20 to produce maps, tables and graphs that helps to visualize, analyze and interpret data.

1.6 Limitation of the research

Due to the limited capacity of the laboratory The XRF result does not include any Rare Earth Elements (REE) and different HFSE that could help to draw more reliable interpretation related to original tectonic setting of the rocks.

In addition, the laboratory can analyze only seven elements using AAS technique; that means the laboratory is unable to analyze multi-elements especially the pathfinder elements for gold.

The other limitation of the study is restriction by the company to geological report, maps, assay result and access to all drill holes. The analysis and the conclusion would have been sounder, if the mentioned data had been used.

1.7 Previous works

The presence of gold in Ethiopia has been known for centuries (at least 3500 years) and recorded by historians through evidence that early Egyptian Pharaohs conducted commercial expeditions to the region trading of gold, ebony, myrrh and incense with Ethiopia (Golden star 1996). Since that time, artisanal mining of placer gold at river beds has continued in many regions (Golden Star Resources Limited, 1996). Regional scale mineral exploration and mapping projects in the past have been conducted by the Geological Survey of Ethiopia (GSE) formerly known as the Ethiopian Institute of Geological Survey (EIGS). Efforts by EIGS to produce 1:250,000 geological maps all over Ethiopia, including Kurmuk-Asosa sheet.

The western Green Stone Belt (GSB) has been well known for its gold occurrences since 1930's. Historically the belt has been prospected for primary gold and associated base metals mineralization. The presence of old Adits at the top of mount Dul (southern extension of Ashashire) and open shafts, winzes and drive at Odonok 55 km NW of Asosa is an evidence for small scale mining in 1930's (Chewaka S, and de Wit, 1981; Jelenc, 1966).

Historical records mention Swiss and Italia-German companies working within the region pre- world war II, prior to and during Italian occupation (Jembere M, 1995). There is little evidence of the work they conducted. The size and number of artisanal workings within the area suggests that they may have been ongoing for a number of years, likely pre-dating the Swiss and Italia-German workings and probably dating back to historical periods. The Proterozoic GSB of western Ethiopia has been regionally mapped and evaluated by Hess (1932) and Fontana (1954). Usoni (1952) compiled a mineral occurrence map of western Wellega.

A photo geological mapping exercise was undertaken by Hunting Geology and Geophysical Limited with Survair Geophysical Limited in 1967 on behalf of UNDP program. Base metals exploration started in 1969 with an extensive geochemical reconnaissance program carried out by the UNDP in the area to the west of the Blue Nile. A joint EIGS-UNDP mission conducted mineral exploration surveys from 1967- 1971. The mineral exploration survey included airborne radiometric and magnetic surveys (UNDP, 1972).

The Metal Mining Agency of Japan (MMAJ) conducted two phases of exploration between 1973 and 1974, with the aim of outlining the mineral occurrences and geology (MMAJ, 1974). As with UNDP work, the MMAJ first carried out a photo geological reconnaissance survey at 1: 50,000 to 1: 60,000 scale and geochemical prospecting (stream sediment, pan concentrate, and soil sampling). The work was focused on three zones designated A, B, C which incorporates Asosa-Kurmuk-Gizen, Mendi-Tobo and Billa areas respectively which totally covers 10,000 km^2.

Between 1980 and 1982, the EIGS completed a program of stream sediment, soil and rock sampling together with the re-interpretation of previous work (Ahmed M, 1982). This work was conducted with the aim of finding area of interest for follow-up work which was to include geological mapping, geophysics, soil, rock, and drill core sampling (Ahmed M, 1982).

Between 1982 and 1983, the GSE conducted follow-up work on from their earlier survey, with regional surveys, including 2,772 soil samples from a number of detailed 100m by 500m grids and 225 rock samples taken from altered or mineralized outcrops to supplement the soil grids (Jembere M, 1984). This work delineated a number of anomalies within Dul Mountain, Azale and Ashashire targets (Jembere M, 1984).

Golden Star Resources Ltd (1996) undertook a systematic Bulk Leach Extraction of Gold (BLEG) soil sampling over an area of 16 km^2 with a surveyed grid of 400m by 40m. A total of 1593 soil samples were collected from "B" horizon and analyzed for gold using BLEG analysis. Geological mapping, soil geochemistry and rock sampling, and seven trenches were hand dug.

Table 1.2 Summary of the work completed by Golden Star Resources at Ashashire target.

Type of work	Unit	Volume	Notes
Trenching	Meters	483	7 trenches
Channel samples	Number	183	
Soil samples	Number	1593	
Grab samples	Number	83	

A total of 83 rock chip samples from various lithologies were also analyzed by fire assay. As a result 1800m long and 25- 30m width, open anomalous zone were defined consisting a narrow erratic zone of quartz vein within a sheared tuffaceous and metavolcanic sequences.

Table 1.3 Best previous assay results from trenching at Ashashire by GSR

Trench	From	To	Length (m)	Au (g/t)
ASHTR1	29.65	43.75	14.1	6.36
ASHTR2	32.85	41.85	9	1.34
ASHTR3	12.1	18.1	6	0.73
ASHTR4	31.65	33.65	2	2
ASHTR5	38	58.85	20.85	2.79
ASHTR7	24.85	38.45	13.6	5.28

Presently, Gold Fields Exploration (Ethiopia) and Benzu Gold Mine Ethiopia PLC are jointly working on detail exploration of further trenching and sampling followed by drilling activity on the main anomalous zone to intersect the proposed ore body. Side by side, regional and detailed interpretation of 400m spaced airborne survey and high resolution 50 m spaced magnetic and radiometric survey was conducted.

CHAPTER TWO

2 REGIONAL GEOLOGY

2.1 The East African Orogen

The EAO (Figure 2.2) is one of Earth's longest Neoproterozoic accretionary orogen and collisional zone within Gondwana (Stern, 1994; Cawood et al., 2009). According to Kroner and Stern (2005) the orogen extends about 6000 Km long that stretches from southern Israel in the north to Madagascar to the south; and it consists of two major segments: the Arabian–Nubian Shield (ANS) in the north, and the Mozambique Belt in the south (Stern 1994; Stern 2002).

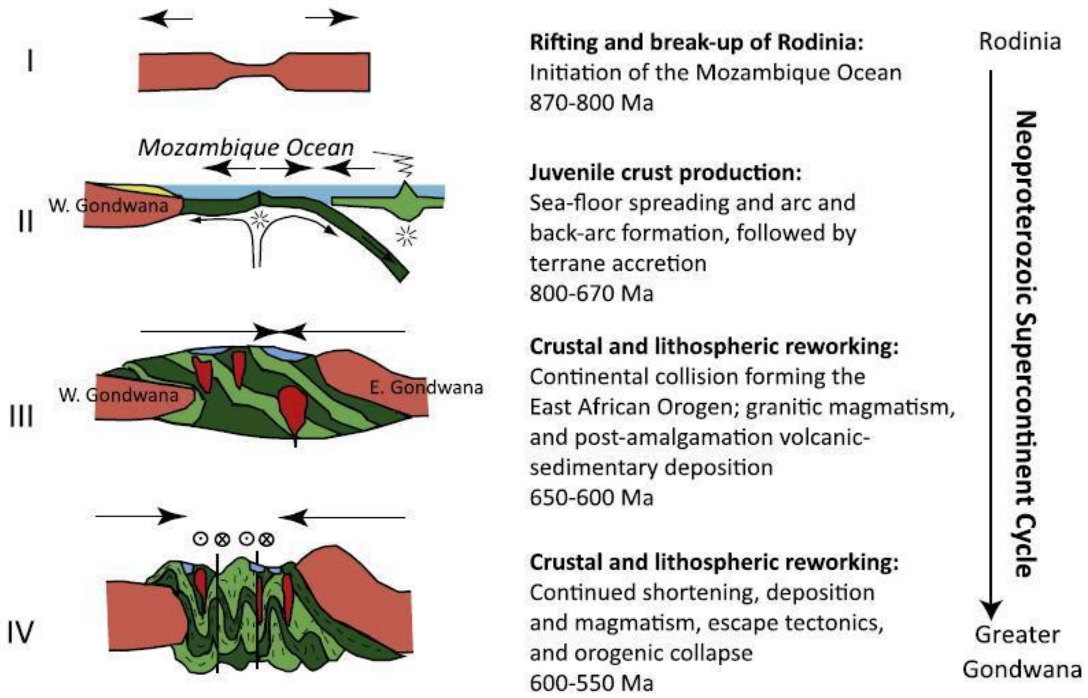

Fig. 2.1. A schematic diagram of the suggested stages of tectonic evolution of the Arabian-Nubian Shield (after Stern and Johnson, 2010 cited in Johnson et al., 2011).

The evolution EAO had taken place over a time period of about 350 Ma between 850 -557Ma and demonstrated a Wilson Cycle orogeny.

The creation of the orogen is the result of the closure of the Mozambique Ocean that is associated with the collision and coalescence of numerous juvenile island arcs terranes and followed by the collision of East and West Gondwana that has finally resulted in the formation of Gondwana Supercontinent (de Wit and Chewaka 1981; Stern 1994, 2002; Kroner and Stern, 2005) (Figs 2.1 &.2.2).

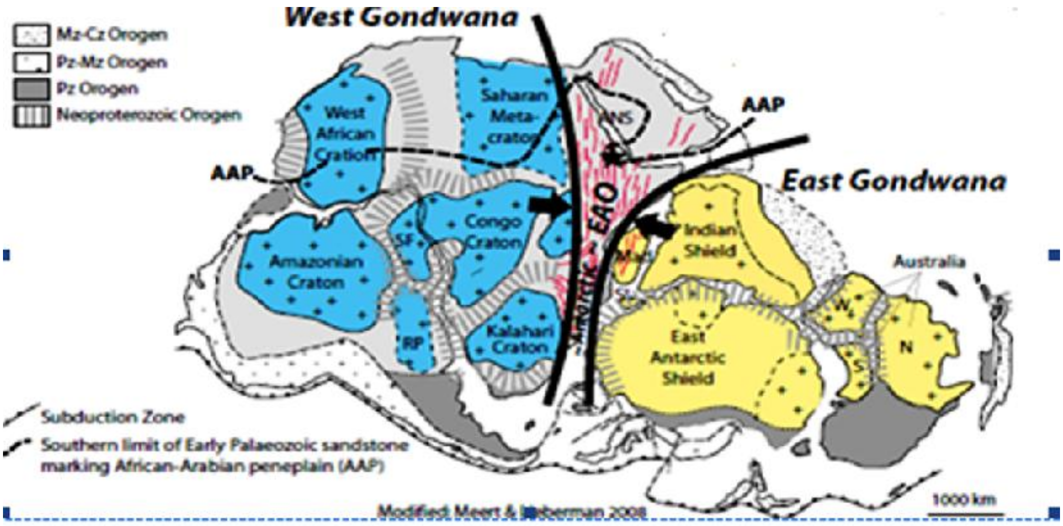

Figure 2.2 Gondwana amalgamation and emergence of the Antarctic-EAO. (After; Meert & Lieberman 2008; Gray et al., 2008). The fig. also shows global palaeogeographic reconstructions for 550 Ma,

2.2 Geological Setting and Mineralization

2.2.1 The Geology of Ethiopia

The Geology of Ethiopia can be grouped in to four major units, namely the precambrian basement, the late paleozoic to mesozoic volcanic and sedimentary succession, tertiary volcanics and sediments succession, and the quaternary sedimentary and volcanic rocks including the evaporates in the rift system. The basement rocks, which are a part of the East African Orogeon (EAO), comprise a wide variety of meta-sedimentary, meta-volcanic and meta-intrusive rocks which have been subjected to variable degrees of metamorphism and deformation. The basement is usually covered by continental and marine sediments of Permian to Paleogene age and by Tertiary to Quaternary volcanic rocks and related sediments. However the exposure occurs in areas of high erosion where the Phanerozoic cover has been removed, in the northern, western, southwestern, southern and eastern part of the peripheral part of the country covering 17% of the landmass.

The country's basement rocks have been studied by a number of scholars, among these to mention some: Kazmin (1971, 1975), Kazmin et al. (1978), de Wit and Chewaka (1981), Ayalew et al.(1990), Tadesse et al.(1997,1999,2000) Alene et al. (2000), Asrat et al.(2001), and Yibas et al.(2002).

Kazmin (1971, 1975) classified the basement rocks of Ethiopia into three complexes.

This threefold division of stratigraphic model was based solely on lithological and structural mapping with little or no geochronologic data. According to his division, the Lower complex (older than 2.5 Ga) formed of high grade gneisses and represent cratonic basement; however, the Middle complex (lower Proterozoic to middle Proterozoic) is composed of metasediment and the upper complex (upper Proterozoic to lower Paleozoic) consists low grade rocks including ophioliitic rocks, andesitic metavolcanics and associated metasediment and to less extent metacarbonates.

The Ethiopian basement is regrouped in to two major lithological terrains according to Asrat et al. (2001) and Yibas et al. (2002). These are:

(i) A gneissic and migmatitc terrain, which essentially consisting of high-grade para and orthogneisses , deformed and metamorphosed granitoids, previously known as the Lower and Middle Complex (Kazmin 1971, 1975), and correlated with the Mozambique Belt;

(ii) A low-grade volcano-sedimentary terrain, the ophiolitic fold and thrust belts, which comprises all the rocks of the Upper Complex and is correlated with the ANS (Fig. 2.3).

Pre-syn-, and post-tectonic granitoids intruded the Ethiopian basement rocks (Asrat et al. 2001).

These two distinct lithotectonic terranes show contrasting lithological association, internal structures and grade of metamorphism (Yibas, 2000; Yibas et al., 2000a; Asrat et al. 2001).

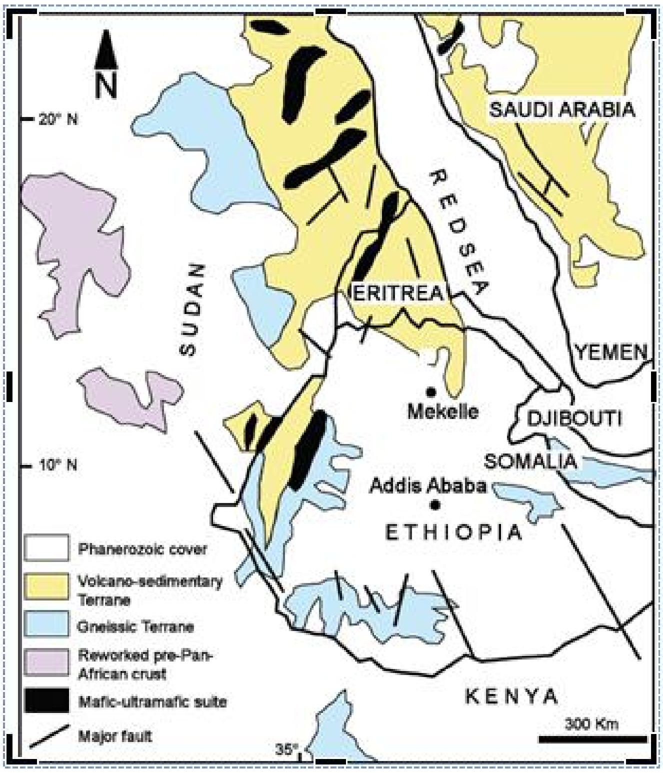

Figure 2.3 Distribution of rocks of the Arabian-Nubian Shield and Mozambique belt, which form the basement rocks Arabian Peninsula,northeast Africa (Egypt and Sudan), and Ethiopia (modified from Ayalew et al. 1990; Asrat et al.2001).

2.2.2 Precambrian rocks of Western Ethiopia

The Precambrian rocks of western Ethiopia that extends northwards from 6^{o}N for about 650 kilometer is the largest Precambrian block in the country (Alemu and Abebe 2000). It forms the western and wider branch of the low-grade volcano-sedimentary terrain package of the Arabian-Nubian shield (ANS) bounded both to the east and to the west by the gneissic terrain of the Mozambique Belt (MB). The sequence is invaded by pre-, syn- and post- intrusions of peridotite,-gabbro-diorite-granitoid composition. Several outliers of Tertiary basalt units are distributed through western Ethiopia green stone belt (WEGSB), along with local alkali stocks and plugs which form impressive topographic features.

The regional geology of WEGSB appears to be relatively poorly documented and understood. Geological maps with scale of 1:250,000 has been completed; however regional geophysics (gravity, aeromagnetics, radiometrics) and reliable U-Pb geochronology is lacking. However, some geochronological data indicate that the gneissic rocks and the metavolcano-sedimentary and mafic–ultramafic sequences of western Ethiopia have similar ages and evolved between 900 and 500 Ma (Abraham, 1989; Ayalew et al., 1990; Kebede and Koeberl, 2003).

The WEGSB trends N-S to NNE-SSE and has been subdivided, east to west, into five litho-tectonic domains these are referred to as: Didesa Domain, Kemashi Domain, Dengi Domain, Sirkole Domain, and Daka Domain (Allen, A. and Tadesse, G., 2003) (Figure 2.4).

According to them the Didesa and Deka Domains represents the east and west of the shield, are characterized by intensely folded fabrics with a more complex structural history reflects a pre-Pan African history, as well interpreted as pre-existing continental fragments.

Kemashi Domain is a narrow 10-15 km wide strip, west of Didesa domain, elongated parallel to Tulu-Dimtu belt, comprises low grade meta-sediments rocks of marine origin, including pelagic sediments, cherts and quartzites interlayered with ultramafic to mafic metavolcanics rocks intruded by ultramafic to intermediate plutons. This domain was interpreted to reflect an ophiolitic terrain representing an arc/ continental suture zone.

Dengi Domain is structural zone that includes calc-alkaline rocks in the central part. It is interpreted to be an island arc exposed at different erosional level. Some of the rocks of this structural zone have got lithological similarities with Didesa domain (Zone-1) in the east. Kazmin interpreted this as island volcanic complexes that were formed from the fragments of the eastern continental mass rifted and moved westward. The presence of ignimbritic rocks at eastern margin of this domain was interpreted to be the result of the early silicic volcanism of opening rifts. Finally, the arc was assumed to be moved back to eastern continental blocks and consequently compressing the oceanic crust and associated sediments of the marginal basin, kemashi domain (Zone-2).

The Sirkole domain which hosts the Ashashire prospect occupies the western portion of the belt and extends in to Sudan. The contact with the Dengi Domain, to the east is not exposed. Rocks of this domain comprises a number of N-S elongated blocks, each a few km wide, composed of moderate grade poly-deformed and metamorphosed gneisses, alternating sequence of low to moderate grade psammitic meta-sediments and mafic to felsic metavolcanics rocks intruded by deformed and undeformed granitoid plutons. This domain is thought to represent an imbricated basement cover thrust-nappe complex. At Ashashire, talc-carbonate altered ultramafic rock are exposed on high way cutting, and appear to comprise a fault bounded block thrust into the surrounding volcano-clastic sediments.

Summarizing the studies of Braathen et al. (2001), Allen and Tadesse (2003) and Johnson et.al (2004), it is concluded that four major deformations are recognized throughout the WEGSB.

Four episodes of deformation have been recognized in the Precambrian rocks of western Ethiopia. Early deformation (D1) is a progressive shortening, which resulted in the development of thrusts and associated recumbent, tight to isoclinal folds with sub horizontal axes and shallowly southeast dipping and north-north-east trending foliations (S1). D2 deformation resulted in steepening of D1 structures into upright folds. D3 deformation represents extensive shortening, which culminated in the formation of major N- and NNE-trending shear zones that are superimposed at high angle to the D1 and D2 structures.

D1, D2 and D3 deformation recorded within the regional structures referred to as Baruda Shear Zone, Tulu Dimtu Shear Zone, Birbir Shear Zone, and Akobo Shear Zone. D4 deformation recorded within the NW-trending Didesa and Surma Shear zones (Figure 2.4).

Generally the Precambrian rocks of western Ethiopia are metamorphosed to green schist facies, reaching to amphibolites facies in some cases (Zubaer, 1986).

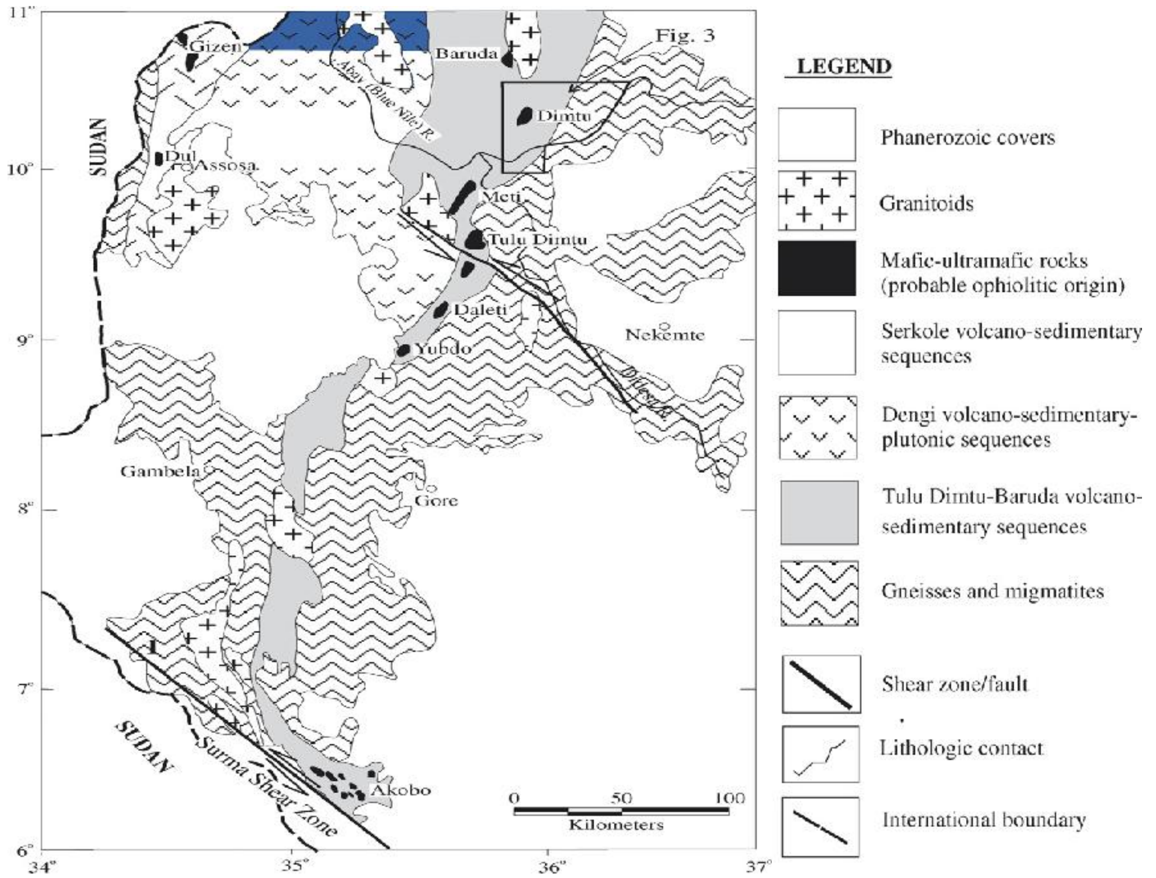

Figure 2.4: Simplified geological map of western Ethiopia differentiating the low-grade volcano-sedimentary terrains and mafic–ultramafic rocks of the Arabian–Nubian Shield and gneissic rock associations of the East-African Orogen (modified from Alemu and Abebe, 2000; Tadesse and Allen, 2005).

2.4 The Regional Geochemistry of Western Ethiopian Shield

The general geochemistry of the western Ethiopia greenstone belt in the Gimbi-Assosa area was described by Allen and Tadesse (2003). Major and trace element geochemistry for metavolcanics have been analyzed using XRF spectrometry from Kemashi, Dengi and Sirkole domains. The Kemashi samples showed range of composition from ultramafic-mafic, the Dengi samples consist from mafic-felsic, and the Sirkole samples comprised from mafic to intermediate. Various geochemical plots have been used to determine the primary chemical characteristics of the lava and tuffs and to delineate their tectonic settings.

The AFM and SiO_2 vs. alkalis plot shows the samples fall within tholeiitic and sub-alkaline fields of basaltic or andesitic composition respectively. The plots didn't show distinction between the domains, most probably due to effect of metamorphic alteration.

The Bivariate plots, to show variation between samples and to identify trends, have been used for SiO_2, Al_2O_3, CaO and Na_2O with MgO. The plots revealed weak negative correlations of SiO_2 and Al_2O_3 with MgO, and a positive correlation of CaO with MgO indicating that magmas evolved by fractionation of clinopyroxene, orthopyroxene and olivine from parent liquids.

Trace element spider diagrams show a tight coherence from the Dengi and Sirkole samples and slight depletion of high field strength elements. Enrichment of Th relative to Nb, and overall enrichment of LFS elements over HFS elements in Kemashi samples are characteristics of ocean floor and back-arc magmas. Ti-Zr-Y tectonic discrimination plot confirms the calc-alkaline basaltic character of the Dengi and Sirkole rocks which developed in convergent setting, while the Kemashi samples fall in the field of ocean floor basalts representing ocean crust material formed in a spreading environment (Tadesse and Allen, 2004).

2.5 Mineral Resources and Mining in Basement Rocks of Western Ethiopia

Western Ethiopia especially the Kurmuk area has been a target for placer and primary gold exploration for many years. The presence of artisanal mining activities suggests that the area has the potential for primary gold mineralization. Some economic minerals other than gold are also found in the basement rocks of western Ethiopia. This includes platinum, copper, iron occurrences of zinc, silver and arsenic is also reported. Beside different rocks that are used for constructing buildings /dimension stones, such as marble and granite, also occur in the region (Tadesse, 2009).

Primary Gold deposit

So far primary gold deposit economic interest is discovered at Tulu Kapi by Nyota Minerals Limited. The gold mineralization at Tulu- kapi is hosted dominantly by a coarse grained intrusive rock i.e altered/albitized syenite. Different projects like Egyptian ASCOM precious metal mining discovered gold deposit, at place called Dish Mountain NW of Ashashire, near to the border town of Kurmuk, but the tonnage was not disclosed yet. Midroc – Gold, a local mining company, has also discovered a skarn –type gold deposit in the Egambo (Bullen district of the region). Besides, encouraging gold and base metals exploration has been undertaken by different companies at Ashashire, Mount Dul, Menghe, Oda Godere, Azale, Ankori, Kata and Boka-Dalleti-Bindakoro prospects.

Gold and sulfide mineralization: In western GSB gold and sulfide mineralization occurs in gossans and ferruginous quartzites and quartz veins hosted in metasediments and volcano-sedimentary sequences. The metals appear to be both lithologically and structurally controlled demanding a firm understanding of contacts and structural orientations. This is due to the fact that the mineralization is confined mainly in low grade GSB near to the contact with high grade rocks. This reflects the litho-structural control of mineralization. There is competency difference between the two groups of rocks which is suitable for the development of dilatant zone and accumulation and precipitation of gold and sulfides.

Platinum: It occurs in wide area mainly associated with serpentinized dunite and pyroxenes. Economic concentration was found in lateritic bed rock called Birbirite. About 2000kg of platinum was exploited in this area up to early 1980’s (Senbeto C. and de Wit, 1981). Two exploration companies: Yubdo Platinum and Gold Development PLC (YPGD) and Western Wellega Mineral Development PLC (WWMD) are working in west Wellega Zone. The YPGD trenching activity showed up to 1.3 ppm in weathered saproloite sections. WWMD is undertaken exploration in 2005, far northern part of western Ethiopia ultramafics at Sirba Abay outcrops in which occurrences of platinum group metals are reported (Platinum potential of Ethiopia by Ministry of Mines of Ethiopia, December, 2010).

Copper: it occurs in wide area mainly associated with gold. Significant values of copper were reported in Keta area and three modes of occurrences were recognized in this area (Jelenc, 1966; Senbeto C. and de Wit 1981).

1) Blue quartz porphyry: hosted in calc-alkaline rocks, the quartz grains are blue in color and porphyritic in texture. Chalcopyrite, azurite, bornite, and malachite are the main minerals.

Copper values range from 550-1300 ppm was reported in this area. (Jelenc, 1966, Stratigraphically related: Chalcopyrite, magnetite, and bornite occurred in bedded iron stone and quartzite. Values of gold 0.5-20 ppm were reported and the origin was believed to be syn-sedimentary.

2) Tectono-metamorphic related mineralization: Chalcopyrite, malachite and pyrite occurred in steeply dipping shear zones in gneissic rocks. Copper values up to 550 ppm were reported overlapping with induced polarization (IP) anomaly.

   Iron: Most of the known iron mineralization in the Basement rocks of western Ethiopia is confined to the eastern part of the Green Stone Terrain. Five places in Nejo-Yubdo area were reported to have hundred thousands of tons of iron approximately with 60 % Fe and less than 0.1 % P_2O_5.

Others: Zinc, arsenic, and silver were also reported associated with gold mainly confined to the Green Stone Terrain.

CHAPTER THREE

3 Geology of Ashashire

As it is shown in the geological map (Figure.3.1) the study area comprises various units with different extent. These include quartz vein, massive granite, plagioclase-muscovite quartz schist/quartzo-feldspathic rock, actinolite-chlorite schist, carbonitized chlorite-sericte-schist and metasediments.

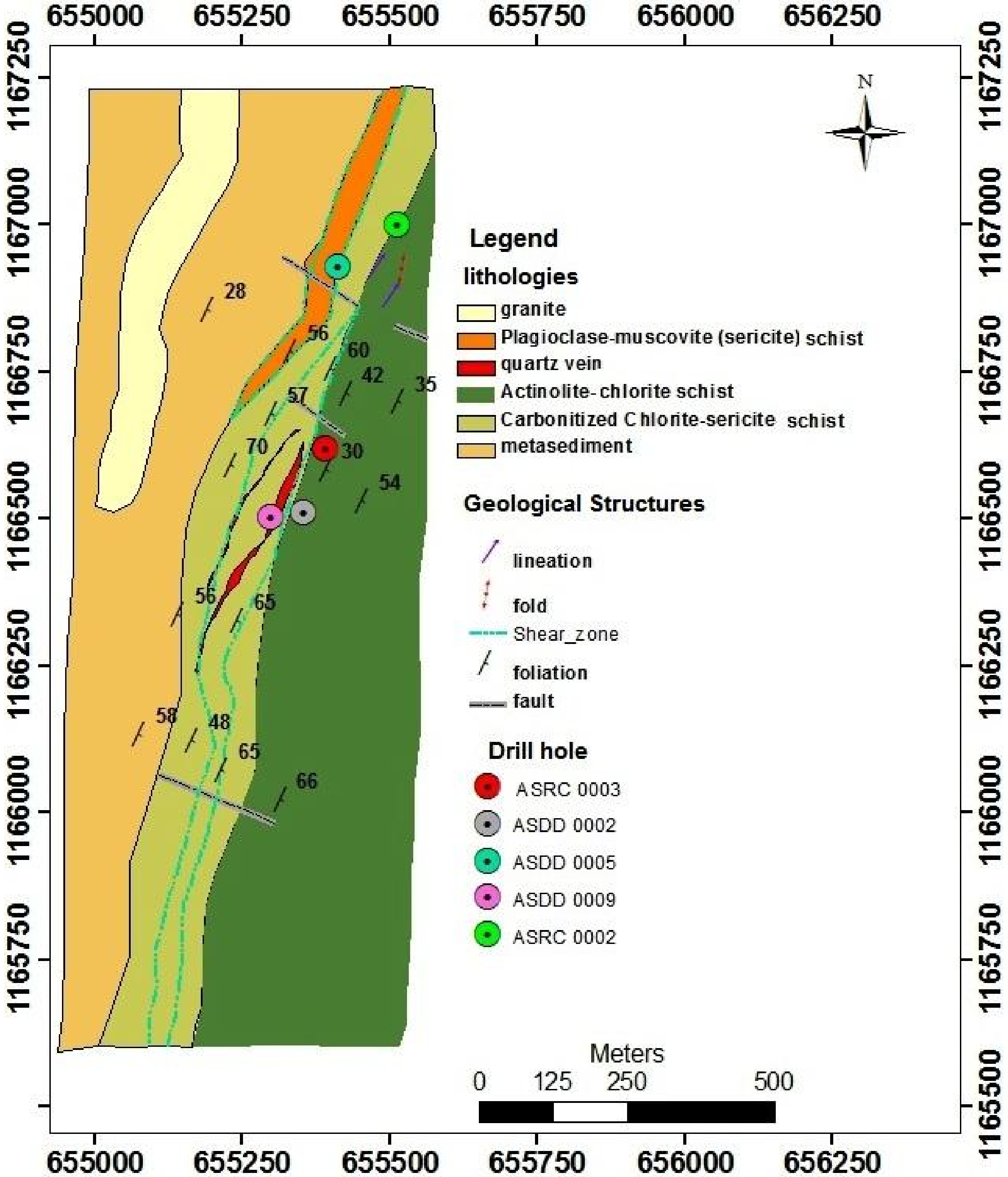

Figure 3.1 Geological map of the Ashashire prospect.

3.1 Granite

The unit is light gray to whitish; massive, consisting of quartz, plagioclase, alkali-feldspar, muscovite and minor biotite. It crops out in the NW part of the study area intruding the metasediment. The unit is texturally massive implying the unit has not been affected by deformational event after it has been emplaced. In other words it is post tectonic intrusive that has intruded the metasediment later than the deformation event.

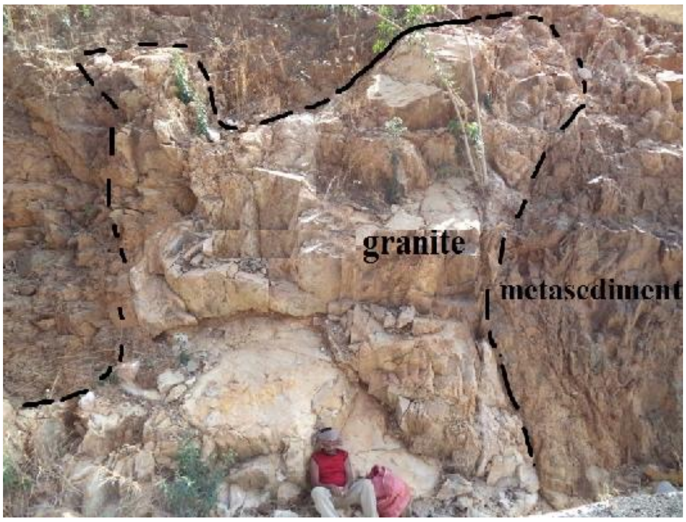

Figure 3.2 intrusion of granitic body in metsediment; note also the sharp contact (black broken line) between the two units.

3.2 Plagioclase-muscovite quartz schist/ Quartzo-feldspathic rock

The unit is composed of sericite/mica, feldspar, quartz and minor biotite characterized by light gray, medium grained, slightly to moderately foliated rock. In many occasions, it is associated with abundant floats of quartz veins. The unit is moderately weathered and exposed at the northern part of the area forming higher topography. It forms sharp contact with the intruded metasediments. Particularly, in the northern most part of the area, the rock is well exposed by road cut, intruding the metasediment /quartz-sericite-chlorite schist indicating the unit is relatively younger than the chlorite schist. It generally strikes NNE 015-030^0 and dips 35-40^0 towards SE.

The Plagioclase-muscovite-quartz schist has been mapped previously as sheared granite.

Thin section study of the representative sample indicates that it is moderately foliated/sheared rock composed of dominantly quartz, muscovite/sericite, plagioclase and opaque (pyrite). Hence it is named as plagioclase-muscovite-quartz schist (Figure.3.3).

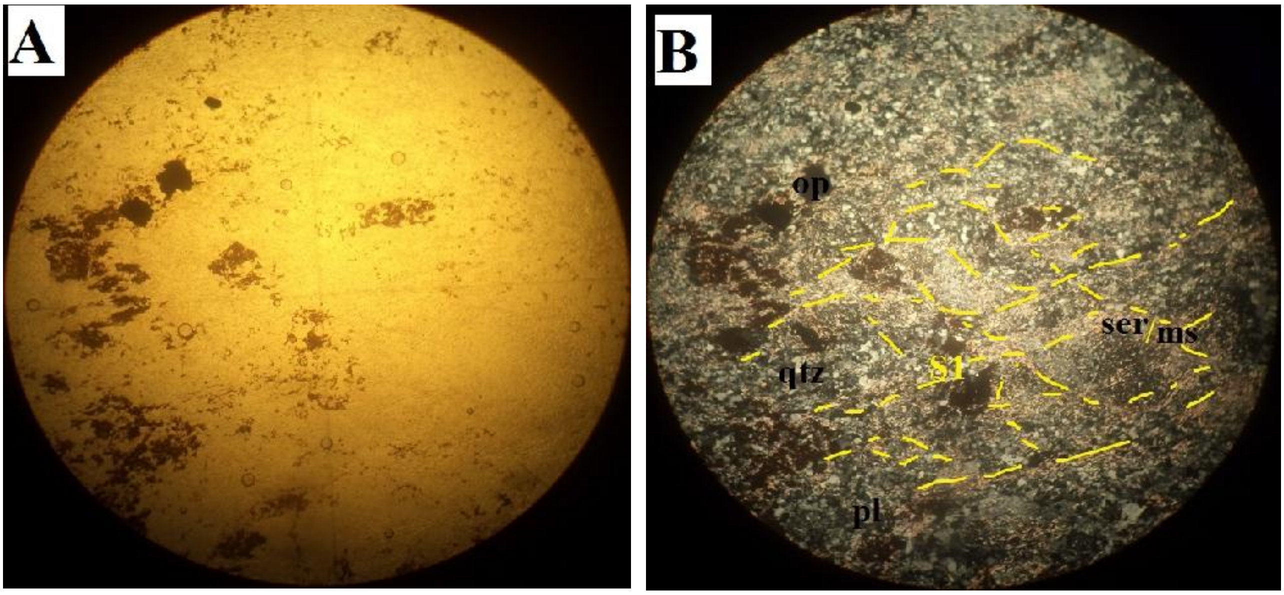

Figure 3.3 photomicrographs sheared granite, location 0655560E, 1167210N.

A. Photomicrograph under PPL , magnification 40x
B. Photomicrograph under XPL, magnification 40x
   Mineral content: quartz 34%, Muscovite/sericite 32%, opaque (pyrite) 16%, plagioclase 15 %, calcite 2%, & epidote 1%.
   Texture and/ or micro structure: Weakly developed s-c fabric (yellowish broken line) is defined by faintly aligned mica minerals that intersect at certain angle..
   Rock name plagioclase-muscovite quartz schist**.**

3.3 Quartz vein

Outcrops of quartz veins are observed at several places in the mapped area (Figure 3.4C). There are also three main types of quartz veins were noted in the area hosted in metasediments and metavolcanics. This includes steeply dipping to the east, flat lying and westerly dipping ones. The quartz veins in general have smoky to white color, glassy texture, and consist oxidized spots and/or box works structures that could be after sulfides. The easterly dipping quartz veins exhibit imbricate structure and appear thicker on surface outcrops. In the middle and southern part of the ridge two major quartz veins dipping to the east and hosted by metavolcanics. These veins are whitish in color, glassy and with box works of weathered sulfides. The host metavolcanics contain pseudomorphs of weathered pyrites and are sheared and altered near the contact with the quartz vein.

3.4 Actinolite-chlorite schist

This unit crops out in the eastern part of target area making a gradational contact with carbonitized chlorite-sericite-quartz schist**.** The fresh rock is greenish; however, it is often found weathered to yellowish color. It is fine to medium grained, well foliated defined by alignment of chlorite and minor sericite. The unit consist concordant and discordant quartz veinlets, mm to 10cm thick, with yellowish oxidized spots and/or vugs probably after sulfide (Figure 3.4C).

At places the schist also comprises cubic oxidized yellowish and brownish spots; with size up to 3mm. Ore microscopic investigation of the fresh representative sample shows that the spots are magnetite. The unit has a general orientation that strike NNE-SSW and dipping to SE. The foliation (S_1) is folded/ crenulated; and caused the development of horizontal crenulation lineations that parallel to the strike of foliation (020^0) (Figure 3.4A).

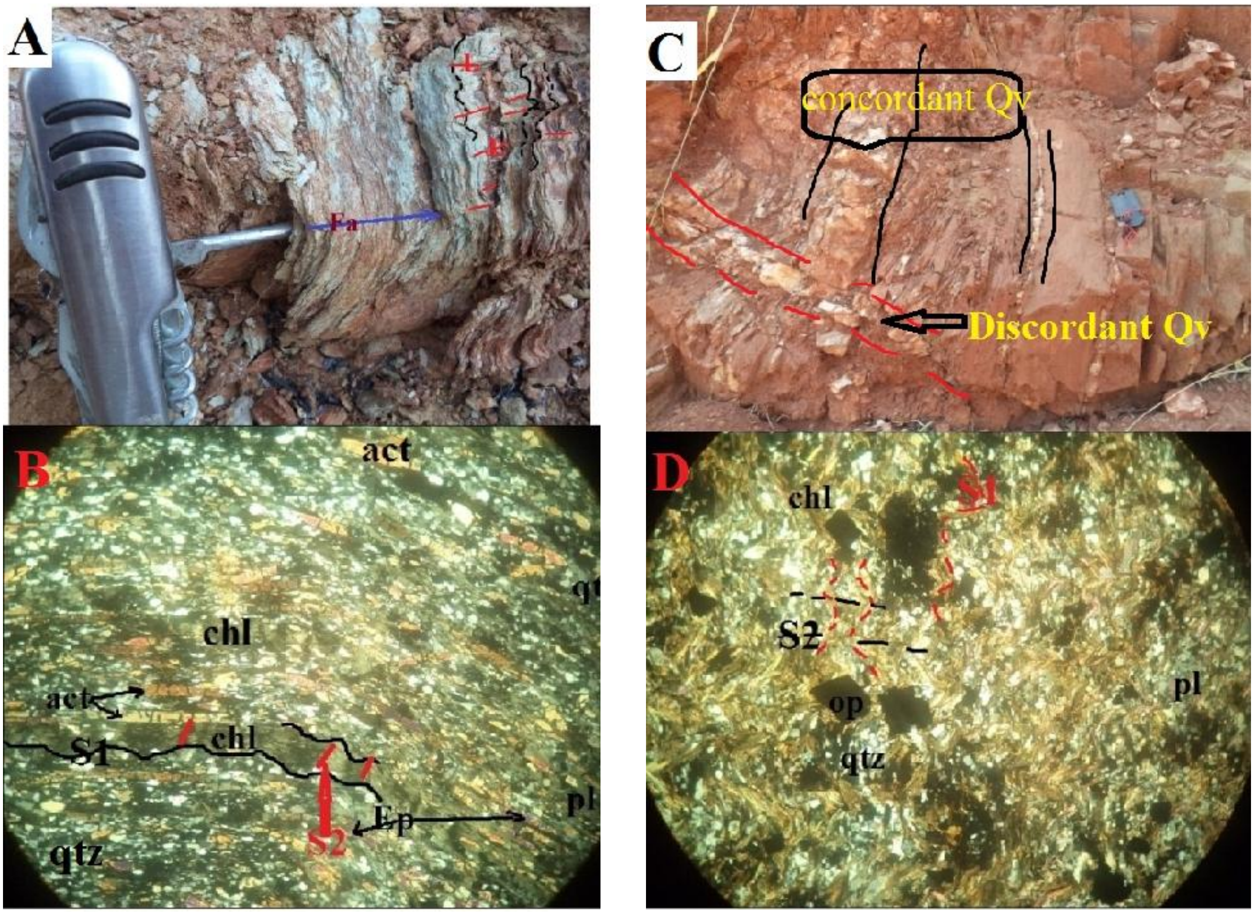

Figure 3.4 Field out crop photo of chlorite schist and the respective photomicrographs.

A. Folded/crenulated out crop of chlorite schist with the horizontal fold axis (blue arrow) that trends parallel to the strike of foliation (020^0). Photo shot, facing north, location 0655582E, 1166910N.

B. Photomicrograph of the sample from A. **XPL,** magnification 40x,
Mineral content: chlorite 26%, quartz 24%, actinolite 19%, sericite 14%, epidote 10% and opaque (magnetite) 3%.
Texture and/ or micro structure: the alignment of chlorite sericite and actinolite define S1 foliation. The S1 foliation has been folded to form S2 crenulation cleavage; particularly in chlorite rich zone, the minerals are realigned to form S2.
Rock name: actinolite-chlorite schist.

C. Out crop of chlorite schist close to the altered zone at the location of 0655629E, 1166742N. The out crop is exposed by road cut that leading to the drill sites. Note that the rock also hosts two generations of quartz vein lets that cross cut each other. The earlier generations are the veins which is concordant to the host. Whereas the discordant quartz vein are the younger and cross cut both host and the concordant quartz vein. It has a trend of $040^0/15^0$NW. photo shot facing south.

D. Photomicrograph of the sample from out crop **C. XPL,** magnificationn 40x**,**
Mineral content: chlorite 33%, quartz 27%, sericite 23%, plagioclase 7% and opaque (mag) 10%.
Texture and/ or micro structure: the alignment of chlorite and sericite define S1 spaced foliation i.e there are micro -lithons consist of quartz and plagioclase between the foliation (red broken line). S2 crenulation cleavage is formed due D2 that folded S1. It is defined by the realignment of chlorite. Note that the opaque minerals (magnetite) simply over print S1 foliation but aligned parallel to S2 implying they had not been affected by D1 but aligned parallel to S2 during D2. Hence, they are intertectonic i.e. they are formed between the two phase of deformation.
Rock name: Sericite-quartz-chlorite schist.

3.5 Carbonitized chlorite-sericite-schist

This unit is the main target of drilling for the gold exploration as it comprises the sheared, altered and mineralized lithologies. It is a narrow zone encountered in the central part of the study area making sharp contact with sheared granite in the northwest part; and gradational contact with metasediment to the west and chlorite schist to the east. On surface exposure, the unit is usually found weathered to pale yellow and/or tan color. From logging and thin section petrology made on the cores from drill holes, particularly ASDD0002 and ASRCD0009, it has been observed that the unit comprises various lithologies with different thickness, degree of alteration and mineralization. The fresh rock has a range of color that is related to the variation in composition and/or alteration; greenish gray, greenish, grayish and at places pinkish; whereas, the altered part appears light gray to whitish.

The lithologies that constitute this unit include metasediment, metavolcanics and minor metamorphosed intermediate to felsic intrusives that are sheared and altered or bleached to different intensity (Figure 3.5). It also hosts various types of quartz vein generations; that are generally concordant and discordant to the foliation. The metasediment comprise various lithologies such as calcite-sercite-quartz schist, chlorite-calcite-quartz schist and quartz-calcite-sericite schist. These lithologies commonly have preserved primary structure which is defined by alternating thin beds/ laminations of calcite, quartz-carbonate, chlorite, quartz-sericite and magnetite minerals that have a range of thickness (0.2-2.0 cm) (3.5A). On the other hand, the metavolcanic, includes calcite-epidote-chlorite schist and quartz-calcite-chlorite schist (Figure 3.5C). Similarly the sheared, altered intermediate and felsic metaintrusives are represented by calcite-quartz-chlorite schist and muscovite-quartz-calcite schist respectively (Figure 3.5B).

Generally this unit is characterized by gray to whitish when they are altered/ bleached that resulted from carbonitazation and sericitization. These altered zones are highly associated with the mineralization; disseminated and/or aggregates of pyrite, chalcopyrite and veinlets of pyrite are abundantly found in the carbonitized and sercitized zone (Figure 3.5A). As a result, this unit is the target of westerly oriented exploration drilling that has been conducted to intersect the mineralized zones. The unit generally trend 010^0-025^0/55-80 SE.

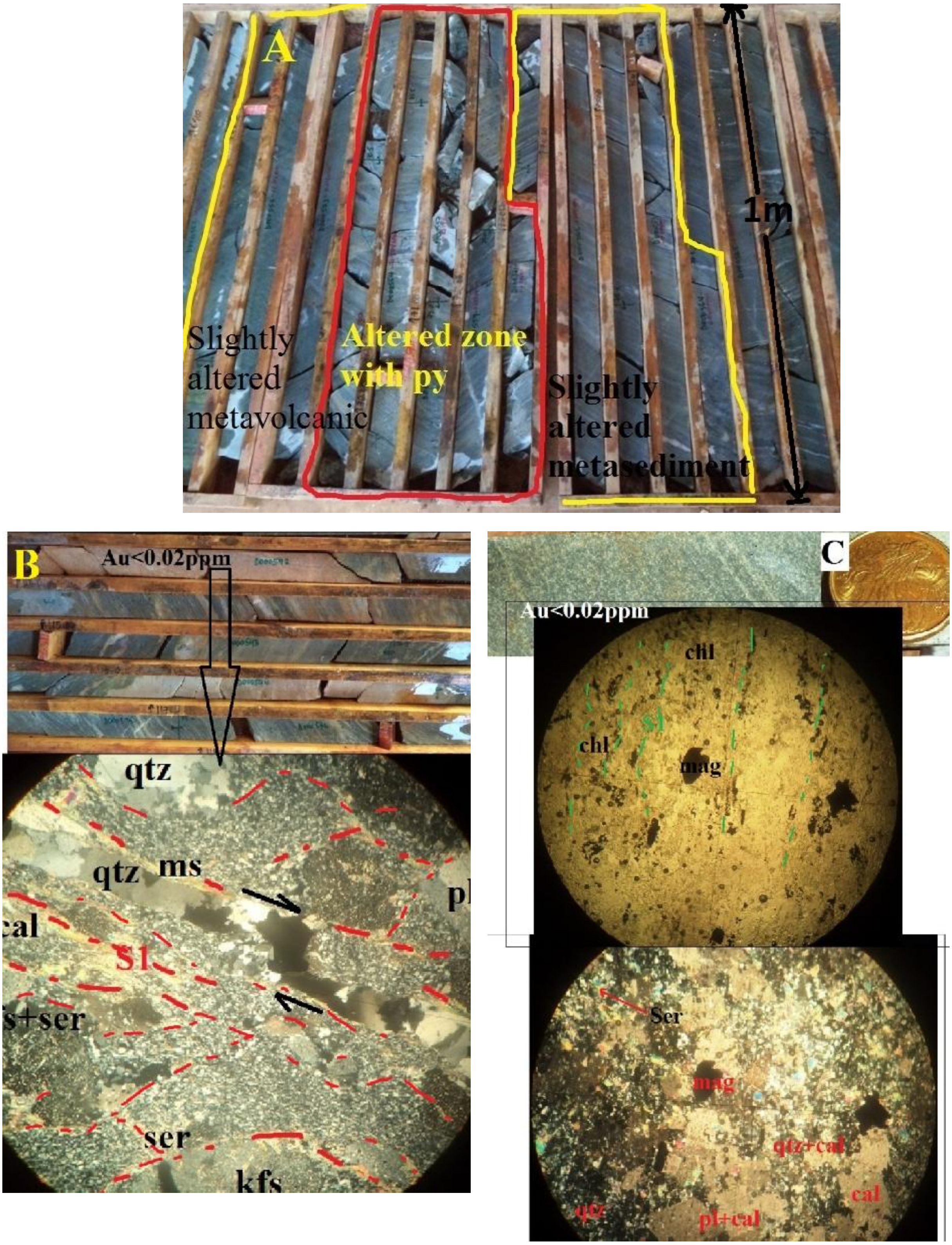

Figure 3.5 Core photos and their respective photomicrographs metavolcanic and metasedimentary rocks

- **A.** Core photo to exhibit the variation between slightly altered and altered (mineralized) zone. It also shows the metasedimentry zone (right) and metavolcanics (left).
- **B.** Core photo (top) is to show the carbonitized chlorite-sericite schist unit that also comprise various sheared

lithologies: metavolcanic, metaintrusives and metasediments. In the picture the sheard metaintrusive (pinkish rock with Au<0.02ppm) makes sharp contact with sheared unit/ chlorite-calcite-quartz schist.
Photomicrograph of the sheared pinkish felsic intrusive (indicated by the black arrow, bottom) and **its** sample number is ASDD002-16, the picture is XPL Magnification 40x.
Mineral content: Mineral content; quartz 37%, plagioclase 30 %, Muscovite/sericite 15%, calcite 10%, opaque 5% & epidote 3%.
Texture and/ or micro structure: the muscovite/sericite minerals define some alignments that form weak s-c fabric. The quartz vein let at the center show a shear sense that implies the rock has experienced local shearing.
Rock name: calcite-muscovite-plagioclase-schist.

C. Core of slightly altered and sheard metavolcanic with its Au value (upper most) and its respective Photomicrographs; sample ASDD002-4A, in PPL (top) and XPL (bottom). Magnification 40x
Mineral content: chlorite 24%, calcite 22%,quartz 20%, Muscovite/sericite 14%, plagioclase 10 %, opaque (mag) 6% & epidote 4%.
Texture and/ or micro structure: weakly developed disjunctive S1 foliation (green broken line) is faintly defined by the alignment of platy chlorite.

Rock name: calcite-chlorite schist

3.6 Metasediments

The unit occurs in the western portion of the study area covering larger area relative to the rest of the units. It is grayish to grayish green and weathered to pale yellow. It consists of intercalated various lithologies of different thickness, that includes slate, calcite-sercite schist and calcite-chlorite schist. At places, minor metabasic rocks such as epidote-chlorite schist and plagioclase-calcite-chlorite schist are observed within the unit. As they are more weathering resistance than the metasediment they occur forming relatively higher topography. These lithologies are also intersected by drill hole ASDD0005.

The metasediment is weakly mineralized consisting disseminated magnetite, pyrite and minor chalcopyrite and at times fracture filling pyrite. Hence it is less important in terms of mineralization. Generally the unit is metamorphosed to green schist facies; and also affected by deformation that is manifested by the development of slaty cleavage and schistosity. The schistosity and slaty cleavage has a general orientation of $010^0/32^0$SE. Preserved primary geological structures such as bedding and laminations commonly observed elsewhere in the unit. These primary features are defined by alternating beds/lamination of chlorite, quartz-carbonate sericite, magnetite and at times graphite (Figure 3.6).

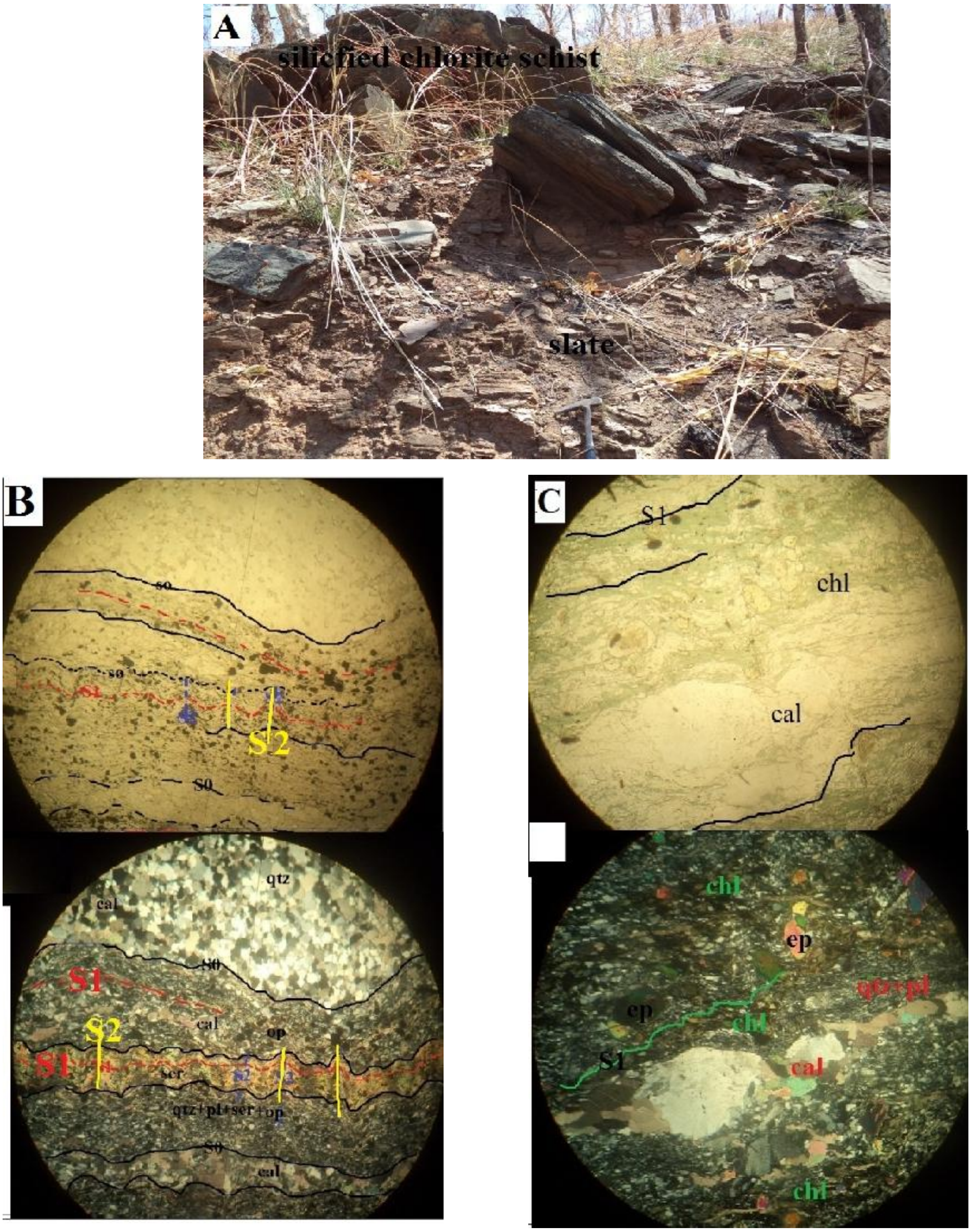

Figure 3.6 A) out crop of metasediment and intercalated silicified chlorite schist in slate. Photograph taken facing west. Location 0655297E, 1167021N.

B) Photomicrographs of the metasediment, sample ASDD0002, in PPL (top) and XPL (bottom). Magnification 40x.

Mineral content; quartz 30%, mica/sericite 25%, calcite 20%, plagioclase 10 %, opaque (magnetite) 10%, chlorite 5% and trace apatite.

Texture and/ or micro structure: trace of bedding (S0 depicted by black line) clearly defined by compositional variations that have different thickness and color. The beds also have planar shape. Generally the various laminations/beds comprised different minerals such as calcite-quartz rich zone (upper most and bottom), calcite-sericite-quartz and opaque/magnetite rich zone (middle) and micaceous/sericite rich zone the yellowish colored part. The bed is affected by two phase of deformations that are manifested by the formation of S1 and S2. S1 (red line) is

a spaced foliation mostly, and runs parallel to the bedding and hence it can be called composite foliation. Whereas S2 (yellow line) is crenulation cleavage that formed due to the micro folding/crenulation of S1 caused by D2. The S2 is more pronounced in this zone due to the compositional variation.
Rock name: Calcite-sericite/muscovite-quart schist.

C) Photomicrographs of epidote-quartz-chlorite schist that named as silicified chlorite schist in the field, sample at way point 509, in PPL (top) and XPL (bottom). Magnification 40x. Location 0655297E, 1167021N.
Mineral content; chlorite 30%, quartz 29%, epidote 15%, plagoclase 13 %, calcite 12% mica/sericite 25%., opaque (magnetite) 1%.
Texture and/ or micro structure: the sample shows well developed disjunctive S1 foliation which is defined by the platy chlorite wrapping around the xenoblastic quartz, plagioclase and calcite minerals.

Rock name: Epidote-quartz-chlorite schist.

3.7 Deformation and metamorphism

3.71 Deformation Structures

Field and thin section investigations reveal that the majority of the lithologies in the study area have experienced various phase of deformations which is manifested by the formation of superimposed secondary ductile and brittle structures. These secondary geological structures include foliations, minor folds, crenulation lineation and fault.

S1 foliations**,** which are associated to D1, are the predominant and characteristic feature of the majority of units in the area. These foliations are defined by schistosity, the alignments of platy minerals such as chlorite, mica and/or sericite, bandings and slaty cleavage. The bandings are clearly shown by alternating layers/laminations of different color minerals that resulted from the variation in composition. Spaced and continuous cleavages are the common type of S1 foliation in the area, the foliations are parallel to relict of bedding (S0), and described as composite fabric. The foliation shows some variation in trend from N-S to NNE (003-025^0/ 30-70^0 E or SE or) (Figures 3.3, 3.5 B &C, & 3.6,**).**
Ductile shear fabrics associated with N to NNE-striking S1 foliations, are observed in various drill holes and in certain outcrops. At places the shear fabrics are overprinted by crenulation cleavage and related kink bands (Figure 3.7).

The small out crop scale folds are the other ductile structures formed by the folding of S1 foliation (Figure 3.3A). They are recumbent type fold with, axial plane trending generally NE and moderately dipping toward NW i.e. 035^0/42^{0}NW and, fold axis plunging horizontally/sub horizontally (0-5^0) to ward NE (020^0). These folds are more commonly observed in chlorite schist than any other units in the area. The lineations that commonly observed on S1 foliation is crenulation lineation (Figure 3.3A). It usually runs parallel to the fold axes. Hence, it is interpreted that both the fold and crenulation lineations are caused by weak second phase of deformation (D2) that folded the S1 foliations.

Figure 3.7 Core photos to show sheared rocks showing well developed shear fabrics i.e. shear bands and associated kinking.

A. Drill core photo showing ductile shear fabrics and sub-horizontal crenulation cleavage with folds in foliated quartz-magnetite-actinolite schist/ altered volcanoclastic sediment. Drill hole ASDD 0009.
B. Well- developed shear band/compositional banding in carbonate-quartz-magnetite-chlorite schist in ASDD 0002.
C. Core photo showing well developed shear band and S-shape shear sense indicator in the far end corner, in quartz-chlorite-magnetite-actinolite schist; drill hole ASDD 0002.
D. Shear band over printed by later folding which is associated with D2; ASDD 0002.
E. Sheared/brecciated and altered rock composed of carbonate, quartz and green mica. Note the disseminated yellowish minerals are dominantly pyrite, and minor chalcopyrite.

The faults are the youngest brittle structure that could be correlated with the later phase of deformation D3.The three east-west trending faults that has been shown on the geological map are identified by the previous work (Golden Star Report, 1996).

However, during the field work small/micro faults has been observed both in the out crop and cores that could be related to the larger ones (Figure 3.8). For instance at the location of 0655542E,1166817N micro fault which displaced 2.5cm thick quartz vein let dextrally by 8cm is encountered (Figure 3.8A). The fault plane is vertical and trends 122^0.

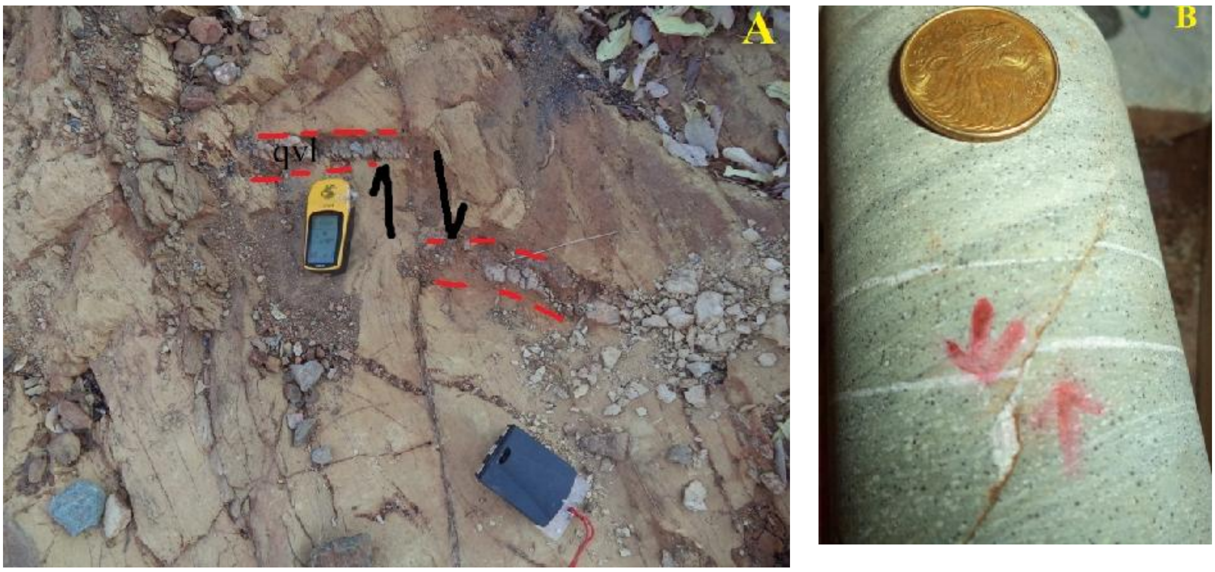

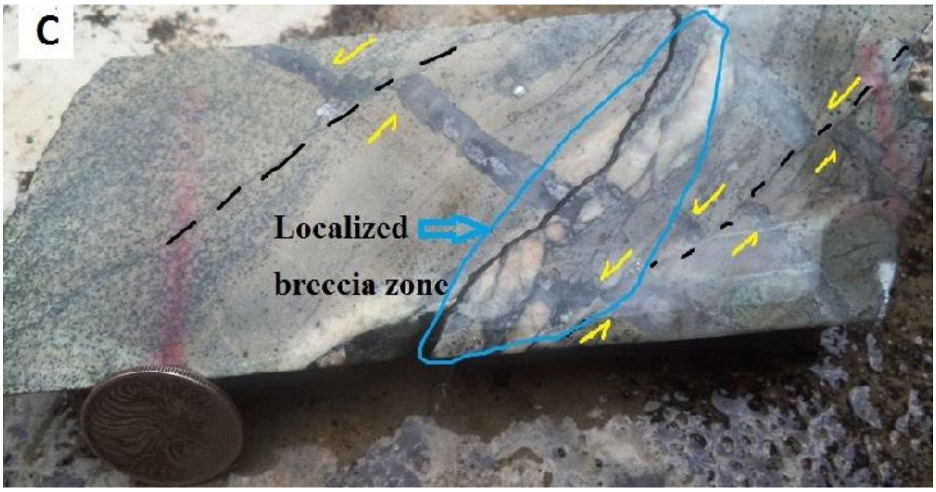

Figure 3.8 small / centimeter scale fault in out crop and core.

A. Small/ centimeter scale fault that displaced 2.5cm thick discordant quartz veinlet in weathered metabasic rock. Picture shot from the top (plan view), location 0655542E, and 1166817N.
B. Centimeter scale fault displacing 2mm quartz-carbonate vein in drill core ASDD0002 at 25.5 m depth. The rock is metadiorite, moderately foliated consisting disseminated magnetite.
C. Bleached/altered brecciated core with disseminated pyrite and faulted grayish quartz veinlets. One of the typical ore zone rocks. Drill core ASDD0002

3.8 Metamorphism

Almost all lithologies in the study area have undergone mineralogical and/or textural changes. Obviously this indicates the parent materials were exposed to different temperature, pressure and/or active hydrothermal fluid, from which the rock initially formed.

Hence, minerals constituting the rocks are forced to change texturally and/or mineralogically by formation/growth of new minerals, to achieve equilibrium.

As discussed under the geology of the dominant lithologic units in the mapped area are described primarily in terms of their texture/fabric and the minerals they contain. Texturally, most of the rocks are foliated that is defined by the schistosity, shear banding and slaty clevage. In this regard, the foliations are dominantly defined by the alignment of secondary minerals, i.e. minerals formed from preexisting minerals during metamorphism; these include sericite/muscovite, chlorite, epidote, actinolite, plagoclase and calcite (Figures 3.4 B&D). Accordingly, the metamorphic grade and facies of the rocks in the area can be estimated by using critical (index) mineral assemblage, which forms in a specific range of temperature and pressure or distinctive conditions. Based on the presence of critical mineral assemblages such as chlorite, actinolite, epidote, sericite, and muscovite, it is interpreted that the rocks in the area have undergone low grade metamorphism that generally belongs to green schist facies.

Minerals such as chlorite, actinolite, epidote, sericite, muscovite and some recrystallized quartz are formed during D1 hence they are aligned and defined S1foliations. Therefore, M1 (metamorphic event one) is considered to be contemporaneous with D1 (Fig.3.4 A & D).
On the other hand some minerals like sericite/muscovite and chlorite underwent rotation and define S2 cleavage during D2. Hence S2, folds and associated crenulations lineations could be related to D2 and M2. (Fig.3.4 A & D & 3.6A).

.

CHAPTER FOUR

4 GEOCHEMISTRY

4.1 Major and trace element analysis

The major and trace element result of fourteen samples, Table 4.1, that represent various lithologies with different degree alteration are analyzed using variation diagram, spider diagram and classification diagram.

4.1.1 The variation diagram

The variation diagram is a bivariate graph or scattergram on which two selected variables are plotted to condense and rationalize large volume of numerical information and to show qualitatively the correlation between the major elements (Rollinson, 1993). He also stated that variation can be explained in terms of different geological process such as fractional crystallization, assimilation or contamination of magma, partial melting and element mobility associated with metamorphism and/ or hydrothermal fluid.

The bivariate plots (Fig.4.1) which use $Si0_2$ on the X-axis and other oxides on the Y-axis are plotted to observe the relationship between $Si0_2$ and Al_2O_3 , CaO, MgO, Na_2O and K_2O. From the diagrams the plots of Si02 vs Al_2O_3 and $Si0_2$ vs CaO (Fig.4.1A & B) shows certain correlation that is negative correlation. On the other hand, the graphs of the other oxides (MgO, Na_2O and K_2O) against $Si0_2$ show no correlation (Figs.4.1C, D and E).

In this particular case, to understand the geological process that is the effect of alteration, bivariate plots which use K_2O on the X-axis are plotted (Figure 4.2). The reason why K_2O is selected on the X- axis is that it shows a very good variation in concentration; particularly in samples that are strongly altered and unaltered. Accordingly, the plots of the oxides against K_2O show two opposite correlation. For instance, the graphs of K_2O vs Al_2O_3 and K_2O vs. CaO Figure 4.2 A & B show positive correlation. This can be due the introduction of potassium, calcium, carbon dioxide and water by hydrothermal fluid that resulted seriticization and carbonitization i.e. enrichment of muscovite/sericite is related to the positive correlation of K_2O vs Al_2O_3 and carbonitization for the case of K_2O vs. CaO.

However, the variation diagram of K_2O vs. MgO, K_2O vs. Na_2O and K_2O vs. SiO_2, Figure 4.2 C, D &E display a general negative correlation. This may imply that the major elements (Mg, Na and Si) have mobilized while the host interacted by the mineralizing hydrothermal fluid. As a result, the host rocks are depleted in these elements after alteration. Due to such effects SiO_2 and MgO cannot be used as an index of differentiation.

Table 4.1 XRF analysis data of major oxides and trace elements

Major oxides in percentage (%)										
Sample number	**SiO2**	**Al2O3**	**Fe2O3**	**MnO**	**MgO**	**CaO**	**Na2O**	**K2O**	**TiO2**	**P2O5**
Muscovite-calcite schist	34	17.57	8.49	0.23	7.56	11.95	3.85	2.16	1.36	0.03
calcite-muscovite schist	48.95	12.65	7.24	0.14	7.19	9.65	1.25	2.73	0.22	0.02
calcite-muscovite schist	38.96	14.72	8.65	0.19	8.11	10.88	2.07	3.56	0.55	0.03
calcite-muscovite schist	38.38	17.83	8.82	0.2	6.43	9.33	3.44	2.68	0.92	0.04
calcite-muscovite schist	48.54	14.17	11.67	0.12	4.14	6.09	2	2.55	0.99	0.03
ASRCD0009-09	65.65	12.6	4.25	0.09	2.79	4.04	1.07	2.31	0.72	0.04
Calcite- chlorite schist	45.76	14.28	12.53	0.53	8.61	6.59	3.95	0.2	1.11	0.11
Calcite- chlorite schist	51.94	13.64	8.45	0.14	9.84	6.53	4.13	1.69	0.68	0.05
Plagioclase-actinolite-epidote schist	66	13.68	4.73	0.25	1.77	3.05	5.14	1.86	0.45	0.07
calcite-muscovite schist	70.6	12.46	4.75	0.06	1.82	1.43	6.77	0.18	0.46	0.07
calcite-muscovite schist	45.07	15.32	9.89	0.57	17.33	1.02	1.07	1.68	0.46	0.08
Muscovite-chlorite schist	52.66	12.01	10.14	0.18	10.12	5.24	5.21	0.88	0.27	0.04
Calcite- chlorite schist	47.22	11.79	14.26	0.36	16.26	1.39	0.37	0.12	0.22	0.04
Actinolit-chlorite schist	44.64	13.17	12.12	0.19	7.06	6.52	1.83	0.70	1.36	0.19

	Trace elements in part per millon (ppm)									
Sample number	**Ba**	**Co**	**Cu**	**Mo**	**Nb**	**Pb**	**Sc**	**Sr**	**Y**	**Zn**	**Zr**
Muscovite-calcite schist	330	21	144	3	5	29	15	811	22	92	134
calcite-muscovite schist	336	25	45	3	5	30	13	386	18	77	44
calcite-muscovite schist	344	27	1984	3	5	30	16	445	19	80	57
calcite-muscovite schist	337	16	65	3	5	29	15	461	21	77	91
calcite-muscovite	274	37	28	3	5	26	13	263	18	41	60

schist										
ASRCD0009-09	459	11	38	3	5	37	12	381	24	53	78
Calcite- chlorite schist	439	111	19	3	5	62	12	2	23	17	2
Calcite- chlorite schist	282	50	85	3	5	28	15	110	20	66	67
Plagioclase-actinolite-epidote schist	393	37	55	3	6	31	15	204	21	54	52
calcite-muscovite schist	436	9	22	3	5	39	11	69	31	69	148
calcite-muscovite schist	453	19	18	3	14	41	11	78	30	89	151
Muscovite-chlorite schist	437	16	133	3	5	35	15	30	20	1212	39
Calcite- chlorite schist	347	36	47	3	6	32	16	40	19	68	39
Actinolit-chlorite schist	375	85	414	2	1	35	16	14	19	115	35
Calcite- chlorite schist	306	55	112	1	7	31	17	336	25	95	135

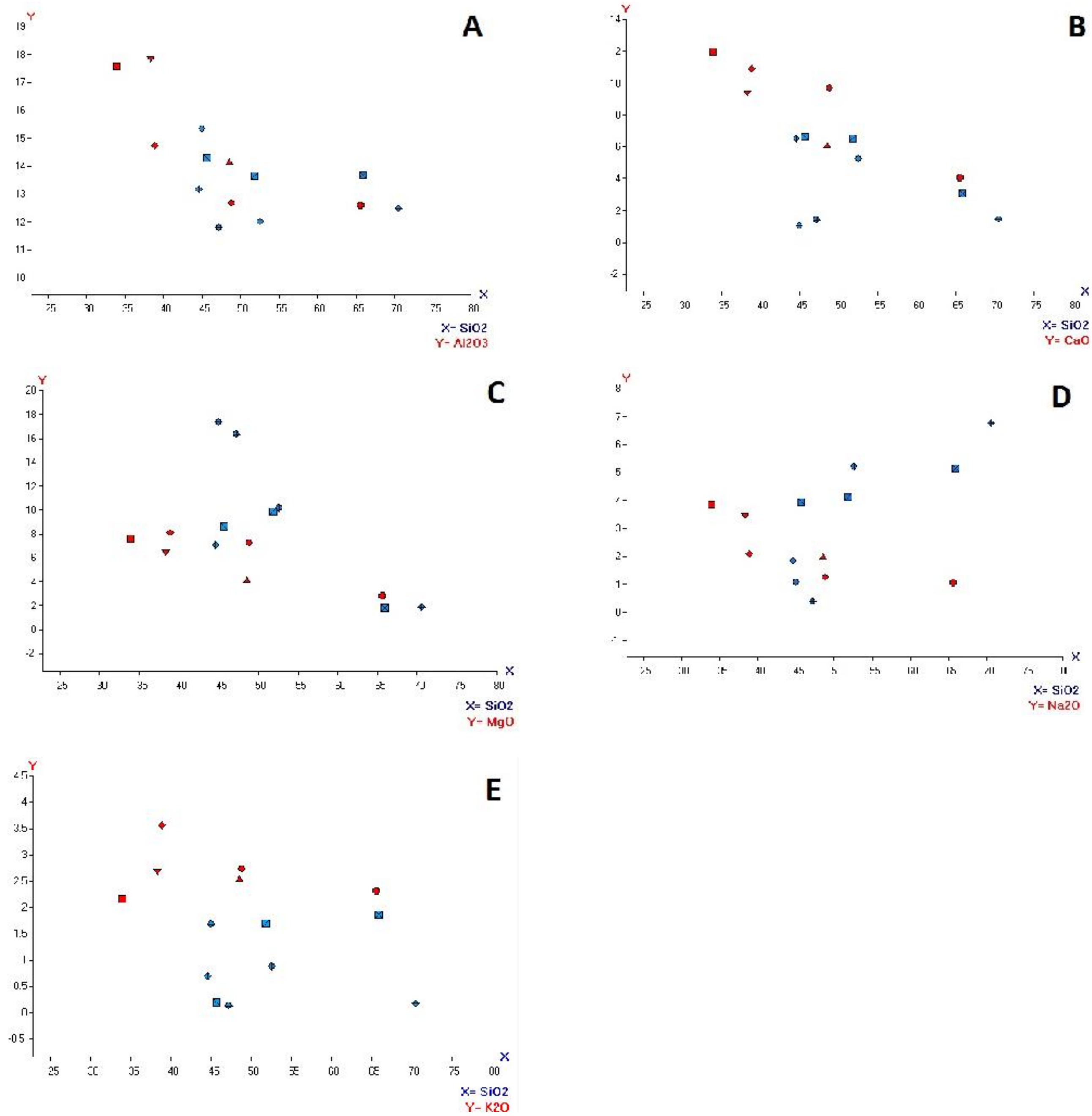

Figure 4.1 bivariate plots which use $Si0_2$ on the X-axis and other oxides on the Y-axis.

A. $Si0_2$ Vs MgO shows negative correlation.
B. $Si0_2$ Vs CaO, shows negative correlation b/n the two oxides i.e. the two oxide decrease simultaneously to the right.
C. $Si0_2$ Vs MgO, displays scattered samples indicating no correlation.
D. $Si0_2$ vs. Na_2O, displays scattered samples indicating no correlation.
E. $Si0_2$ Vs K_2O shows no correlation.

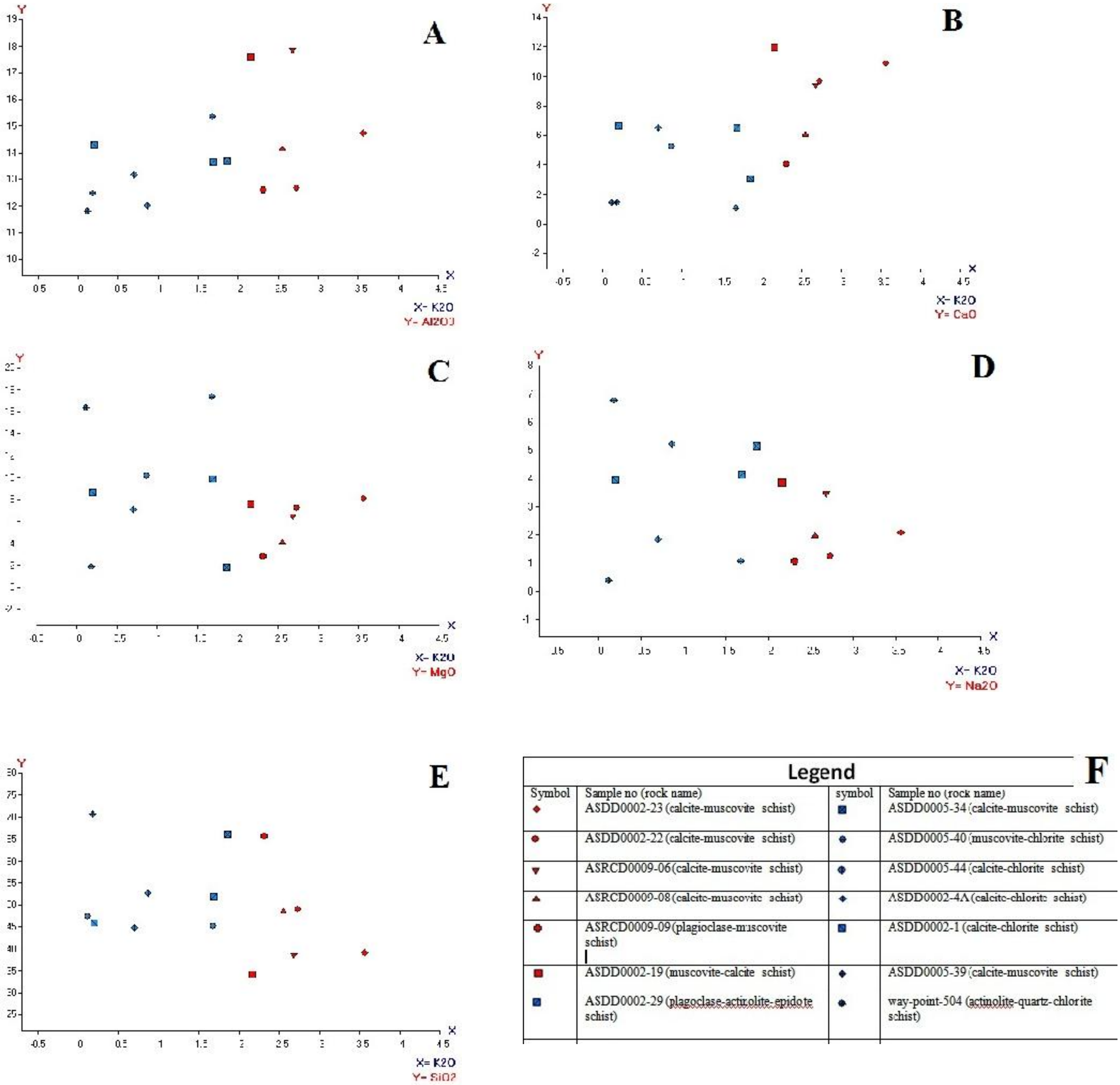

Symbol	Sample no (rock name)	symbol	Sample no (rock name)
	ASDD0002-23 (calcite-muscovite schist)		ASDD0005-34 (calcite-muscovite schist)
	ASDD0002-22 (calcite-muscovite schist)		ASDD0005-40 (muscovite-chlorite schist)
	ASRCD0009-06(calcite-muscovite schist)		ASDD0005-44 (calcite-chlorite schist)
	ASRCD0009-08 (calcite-muscovite schist)		ASDD0002-4A (calcite-chlorite schist)
	ASRCD0009-09 (plagioclase-muscovite schist)		ASDD0002-1 (calcite-chlorite schist)
	ASDD0002-19 (muscovite-calcite schist)		ASDD0005-39 (calcite-muscovite schist)
	ASDD0002-29 (plagoclase-actinolite-epidote schist)		way-point-504 (actinolite-quartz-chlorite schist)

Figure 4.2 Variation diagrams of the samples plotted using K_2O on the x-axis and various major oxides.

Different samples are indicated by various symbols, and altered samples are given red colors and blue for unaltered rocks.

F. K_2O Vs $Al_2O_3$the blue colored samples (unaltered rock) are concentrated in the left lower part of the graph but the altered (red colored) samples are found in right upper part of the graph. This indicates the oxides have positive correlation.
G. K_2O Vs CaO, shows positive correlation b/n the two oxides i.e. the two oxide increase simultaneously to the right.
H. K_2O Vs MgO, displays generally negative correlation with few out layers.
I. K_2O vs. Na_2O, shows negative correlation b/n the two oxides i.e. the two oxide decrease simultaneously to the right.
J. K_2O VsSiO_2shows generally negative correlation.
K. Legend of Figures 4.1,4.2 and 4.3

Note: The oxides are in percentage (%).

4.1.2 Spider Diagram

Spider diagram is a multi-element diagram which is used to analyze the different pattern of trace element distribution that could be associated to hydrothermal fluid, source rock chemistry and/or partial melting (Rollinson, 1993). The spider diagram of the samples (Figure 4.3) from the study area generally shows enrichment of the Large Ion Lithophile Elements (LILE) Sr, K, Ba, also known as Low Field Strength (LFS) or mobile elements. Beside in the diagram the altered samples (shown in red color) have more LILE concentration than unaltered samples (blue). Hence, this could be explained in terms of the effect of hydrothermal fluid that transports these elements, the LILEs, from somewhere else.

On the other hand, the pattern HFS elements Zr, Ti & Y, in the right side of the diagram shows almost no variation i.e. all samples run parallel to each other even if the concentration of HFSEs are slightly lesser in the altered rocks (red) than the fresh unaltered samples (blue). The explanation for this type of pattern could be, the rocks are genetically related or they have similar source rock. On the other hand, the negative anomaly of phosphorous shown by all samples in the diagram is due the presence of little concentration of apatite in the source rock.

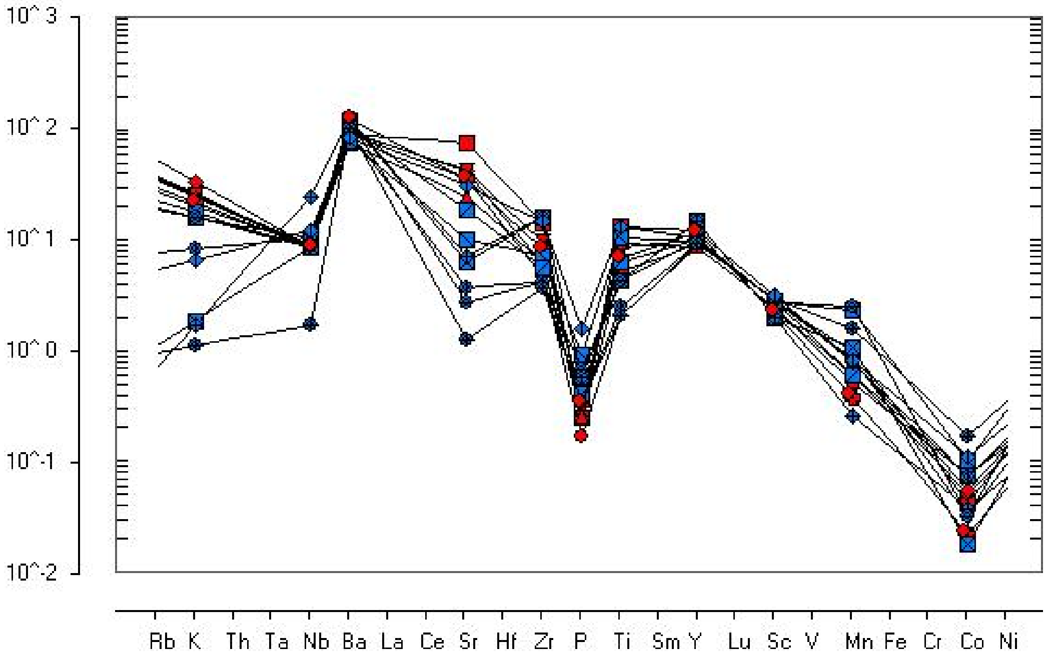

Figure 4.3 Chondrite normalized (wood et al.1979b) spider diagram of analyzed trace elements showing enrichment of LILEs.

The enrichment of LILEs, in the left side of the graph, are higher in the altered rocks (red colored) than unaltered rocks (blue colored) but in the right side of the concentration of HFSEs are generally slightly lesser in the altered rocks (red) than the fresh unaltered samples (blue).

Note: the symbols in the graph is the same as those used in figure 5.3 .Hence, the legend in figure 5.3 can also be used for this figure.

4.1.3 Classification/Discrimination Diagram

Trace element discrimination diagrams are the largest group of discrimination diagrams which can be used to suggest the former tectonic environment of suites of rocks (Rollinson, 1993). According to him, HFSE such as Ti, Zr, Y, Nb and P are usually preferred to construct tectonic discrimination diagrams due to the fact that they are insensitive to secondary processes, insoluble and immobile in aqueous fluids and remain stable up to medium metamorphic grades. The graph Ti Vs Zr, (Figure 4.4) (Pearce and Cann (1973), shows the majority of the samples fall in island arc tholeiites and calc-alkali basalt; and some in mid oceanic ridge basalt (MORB) zone.

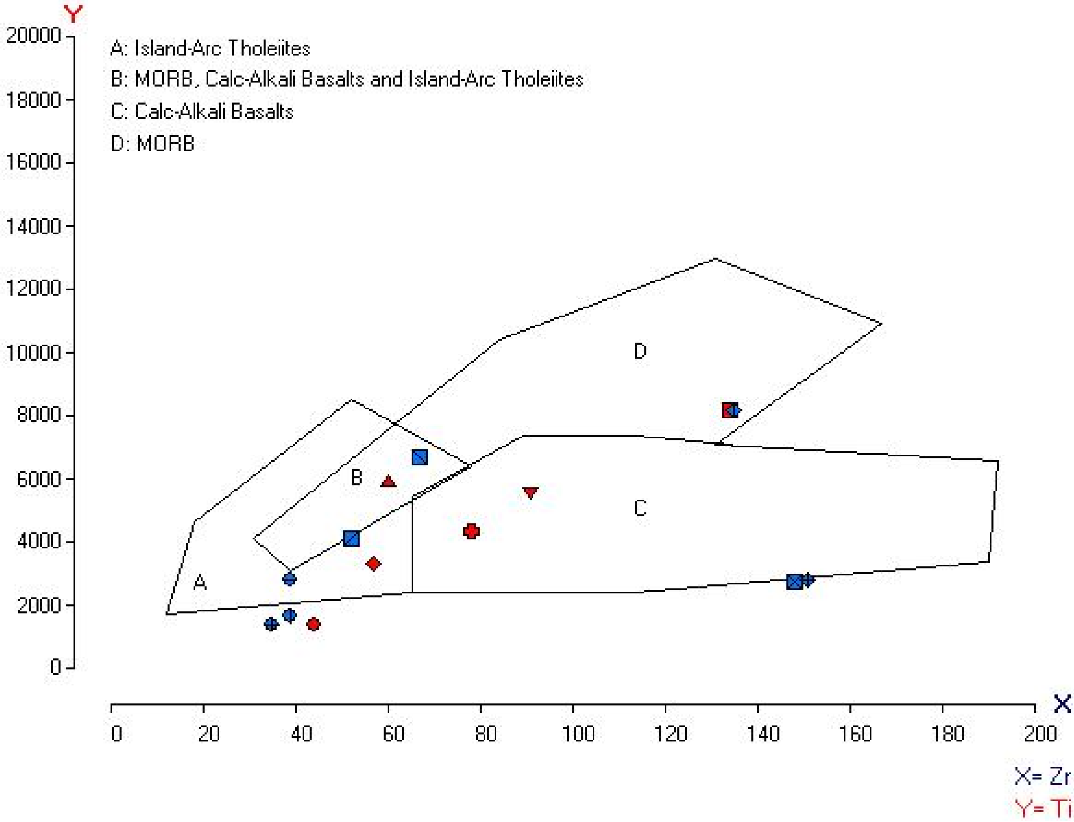

Figure 4.4 discrimination diagram of Ti vs. Zr (Pearce and Cann (1973) exhibiting the majority of the samples fall in island arc tholeiites and calc-alkali basalt.

Note: The legend similar to that of Figure 4.2

4.2 Geochemistry of gold and other metals

A total of 19 core chips and 20 Reverse Circulation (RC) bulk duplicate samples including one quartz vein sample were analyzed for gold, base metals and other metals (Ag, Cu, Pb, Zn, Ni, Co and Mn) using AAS analysis. The result of the analysis is presented in the Annex 1.

The core chips were taken from three drill holes such as ASDD0002, ASDD0005 and ASRCD0009, the RC bulk duplicates are sampled from ASRC0002 and ASRC0003 while the quartz vein sample is taken from surface exposure. Drill-holes samples were taken from different depth based on the variation in lithology, alteration and mineralization.

4.2.1 Analysis of AAS results

The analytical result of the samples, which is calculated using IBM SPSS statistics software version 20, reveals gold concentration from < 0.02-48.5 ppm and mean value of 2.88ppm, (Table 4.2) which can indicate the presence very promising gold concentration in the study area. In the table the value of variability measure such as standard deviation, variance and range are given. The variance (square of standard deviation) and the range are large numbers which indicate the variation between each assay value and the mean is high. Similarly, the range is also high value, implying the difference between the maximum assay value and the minimum is large. Hence the variability measures indicate the analyzed samples have a range of grade from low to high.

Table 4.2, also confirm significant amount of the analyzed data is above 0.5ppm. For instance at 60percentile the value of Au is 0.6ppm that means 60% of the samples have Au value less than 0.6ppm. In other words the remaining 40% samples have anomalous gold value above 0.6ppm. Similarly, the 80th percentile reveals 80% of the analyzed samples have Au value less than 3ppm; i.e. 20% of the samples have more than the average value i.e. 3ppm.
On the other hand, the 10th percentile shows only 10% of the data is below the detection limit of the laboratory, i.e. 0.02ppm.

Table 4.2 Descriptive statistical analysis of AAS results of gold.

Statistics of Au assay result		
Sample No	40	
Mean		2.88
Median		.42
Std. Deviation		8.05
Variance		64.75
Range		48.47
Percentiles	10	<.02
	20	.03
	25	.04
	30	.07
	40	.26
	50	.42
	60	.64
	70	1.38
	75	1.84
	80	2.99
	90	7.41

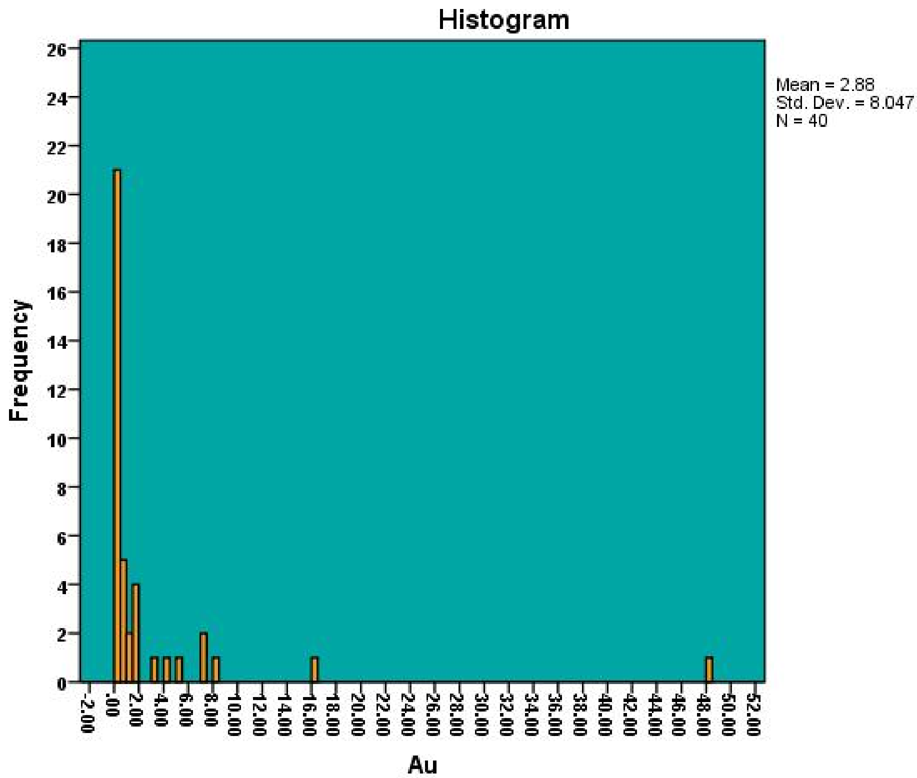

Figure 4.5 Histogram to show the distribution of gold in the analysed forty (40) samples majority from different drill holes and some samples are from out crop.

The right skewed histogram (Figure 4.5) with bar width of 0.5 shows that the concentration of Au b/n <0.02ppm to 0.5ppm has a frequency of 21; indicating about 51 percent of the data lies in this range. In other words the remaining 19 samples (49%) have returned above 0.5ppm. These gold anomalous samples, generally samples with Au value>0.5ppm, are associated to either the altered sulfide bearing sheared zones with quartz vein stringers/ and/ or mineralized quartz vein. Whereas, the samples with assay value less than 0.5ppm are related to weakly and/or unaltered lithologies.

4.2.2 Correlation of Au with Ag, Cu, Pb, Zn, Ni, Co and Mn

The correlation of Au with the analyzed multi elements is summarized in the table 4.3 below, and also displayed by the scatter diagrams (Figure 4.5). The calculated correlation obtained using IBM SPSS statistics software version 20.

Table 4.3 Correlation of gold (Au) with the various metals

		Ag	Cu	Pb	Zn	Ni	Co	Mn
Pearson correlation	**Au**	0.62	0.03	0.48	0.14	0.16	0.34	0.01
Correlated Samples	40 (38 for Pb & 39for Ni)	40	40	38	40	39	40	40
Significance. (1-tailed)		.000	0.427	0.001	0.138	0.160	0.016	0.478

.

The correlation value of Au versus Ag is 0.62 which is greater than 0.5 which is the minimum value needed to say the two elements are strongly and positively correlated. The scatter diagram of Au vs. Ag, Figure 4.6, also shows the general linear increment of the two elements simultaneously. On the other hand, the correlation values of lead (Pb) and Cobalt (Co), are close to 0.5 i.e. 0.48 & 0.34,which implies they have weak positive correlation with Au. The scatter diagrams of these elements with Au also display very weak or little positive correlation.

Likewise, the correlation values of Cu, Zn, Ni, and Mn are almost close to zero, which means the gold in the study area is not correlated or associated with these elements.
In addition, the scatter diagrams, figure 4.6, also confirm existence of very little/no correlation of these elements with the gold (Au).

Generally, the correlation table and the scatter diagrams show that gold has stronger positive association with silver (Ag) than any other metals. This could imply the fluid that transported gold also brought the silver but little amount of Pb, Co, Cu, Zn and Ni. .

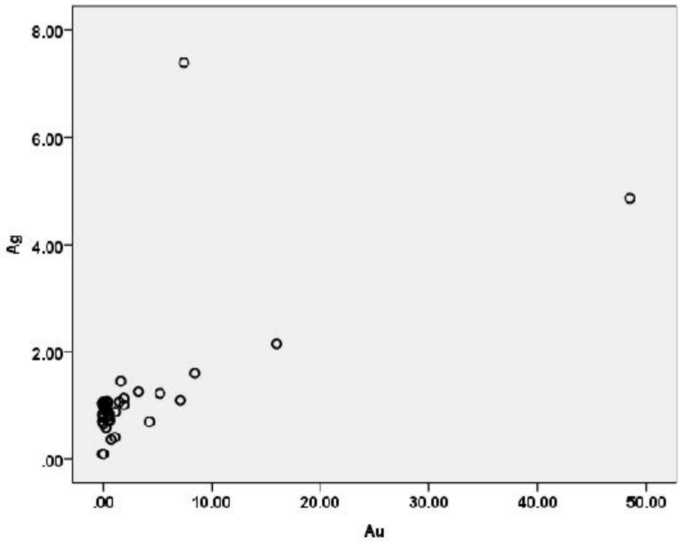

Figure 4.6 The scatter diagram of Au versus versus Ag.

CHAPTER FIVE

5 MINERALIZATION, ALTERATION AND PARAGENESIS

5.1 Ore minerals

Polished sections have been investigated under ore microscope to identify ore minerals and to reconstruct their relative time sequence of formation, i.e paragenesis. Fourteen representative samples were selected from out crop and core to prepare the polished section. Pyrite, chalcopyrite, magnetite, hematite and ilmenite are the identified minerals during the analysis. The results of this laboratory work are presented in Table 5.1

5.1.1 Magnetite and Hematite

Magnetite is the most dominant ore mineral that is found abundantly in the slightly and/or unaltered zone. In hand specimen, magnetite is shiny light gray to black, fine to medium grained; but under the microscope it appears brownish with idoblastic to xenoblastic shape. It occurs crystallized across the section, forming bands, following the direction of gangue minerals such as quartz, carbonate, chlorite, epidote and actinolite, and often replaced by hematite and minor grains of ilmenite; but sometimes magnetite grains also occur as disseminated in the host rocks (Figures 3.2B, 3.3C & 5.1).

The distribution of the mineral is significantly affected by alteration; i.e. the concentration of magnetite dramatically decreases from unaltered to altered zone, whereas the reverse is true for pyrite and chalcopyrite. Hematite is another iron bearing minerals that exist in slightly and /or unaltered zone. Most often hematite is found with the magnetite mostly penetrating the boundary of magnetite, but in very few occasions hematite is also observed having certain mutual boundary with magnetite that may indicate the contemporaneous formation of the two minerals. However the majority data support hematite is formed later than magnetite (Figure 5.1).

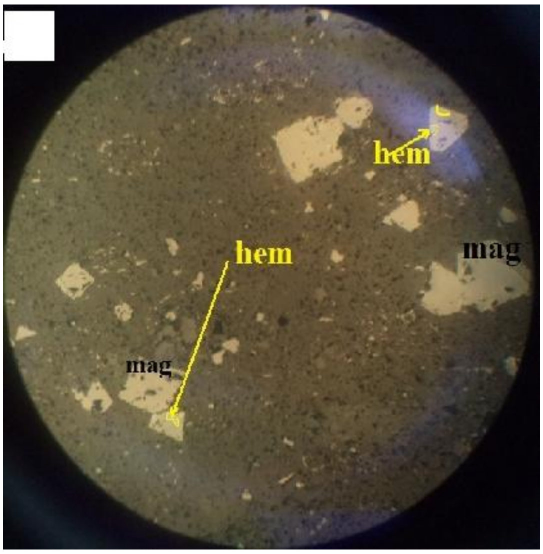

Figure 5.1 Photomicrographs of magnetite and hematite bearing samples that show the relationship between magnetite and hematite.
Sample ASDD0002-02,magnification 100x
Mineral composition: magnetite 30%, Hematite 6%, ilmenite 2% and gangue 62%.
Textural description: As it is shown by the yellowish arrow hematite is found at the grain boundary of the magnetite crystal by replacing/penetrating magnetite. Implying hematite is formed later than magnetite

5.1.2 Ilmenite

Ilmenite ($FeTiO_3$) is the least abundant iron-titanium bearing oxide minerals that found as fine grains replacing magnetite.

Table 5.1 Samples investigated by ore-microscope and their description

Sample no	Mineral	Modal (%)	Texture	**Textural Descriptions / Notes**
ASDD0002-05	Pyrite	20	Idio-Xenoblastic	Spotted and Veinlet texture Veins of pyrite crystallized across the section following the direction of gangue minerals. Inclusions of gangue minerals enclosed on grains of pyrite are poikilioblasts. Microfractures filled by gangue minerals are seen on the grains of pyrite. One fine gold grain masked under gangue is visible in the section. Minor grains of pyrite lie like spot on the gangue minerals.
	Gangue	80	-	
ASDD0002-10	Pyrite	35	Idio-Xenoblastic	Veinlet texture Veins of pyrite crystallized across the section following the direction of gangue minerals. Inclusions of gangue minerals enclosed on grains of pyrite are poikilioblasts. One fine grain of gold is also visible on pyrite grains.
	Chalco pyrite	Trace	Xenoblastic	
	Gold	1grain	Idioblastic	
	Gangue	65	-	
ASDD0002-19	Pyrite	27	Idio-Xenoblastic	Porphyroblastic and Veinlet texture Veins of pyrite and chalcopyrite crystallized across the section following the direction of gangue minerals. Large crystals of pyrite with inclusions of gangue minerals enclosed on grains of pyrite as poikilioblasts are porphyroblast on the section.
	Chalco pyrite	8	Xenoblastic	
	Gangue	65	-	

ASDD0002-20	Pyrite	22	Idio-Xenoblastic	Veinlet texture; Veins of pyrite crystallized across the section following the direction of gangue minerals. Inclusions of gangue minerals enclosed on grains of pyrite are poikilioblasts.
	Gangue	78	-	
ASDD0002-23	Pyrite	30	Idio-Xenoblastic	Replacement and Veinlet texture Veins of pyrite and chalcopyrite crystallized across the section following the direction of gangue minerals. Inclusions of gangue minerals enclosed on grains of pyrite are poikilioblasts. Some grains of pyrite replaced by chalcopyrite and vice -versa.
	Chalco pyrite	12	Xenoblastic	
	Gangue	58	-	
ASRCD0009-02	Pyrite	15	Idio-Xenoblastic	Veinlet texture Veins of pyrite crystallized across the section following the direction of gangue minerals. Veins of gangue minerals are cutting the surface of pyrite grains and micro-fractures filled by gangue minerals are also seen over it.
	Gangue	85	-	
ASRCD0009-05	Pyrite	25	Idio-Xenoblastic	Veins of pyrite crystallized across the section following the direction of gangue minerals. Inclusions of gangue minerals enclosed on grains of pyrite are poikilioblasts. Veins of gangue minerals are cutting some parts of pyrite grains, and micro-fractures filled by gangue minerals also seen over it
	Gangue	75	-	
ASRCD0009-07	Pyrite Gangue	2 98	Hypidio-Xenoblastic	Spotted and Veinlet texture Minor Veins of pyrite crystallized across the section following the direction of gangue minerals. Some grains of pyrite lie like spot in only very small part of the gangue minerals.

5.1.3 Pyrite

Pyrite is the most abundant sulfide mineral in the study area. It is also the second abundant opaque mineral, next to magnetite. In some section, ASRCD009-08, the concentration of pyrite reaches about 65%. The mineral is light yellow with a habit that varies from idoblastic to xenoblastic; and it commonly occurs as disseminated and veinlets; and rarely as massive. Most often, the veins of pyrite are crystallized following the direction of gangue minerals (Figure 5.2C). In a number of cases, it is has also been observed that the pyrite grains enclose inclusions of gangue minerals, giving the minerals poikilioblastic texture which implies the gangue is older than the pyrite (Figure 5.2A). The distribution of pyrite is almost entirely associated with alteration zone. Unlike the oxides, magnetite and hematite, the occurrence and abundance of pyrite is remarkably high in the altered carbonitized and seriticized zone and it diminishes sharply when the alteration dies out.

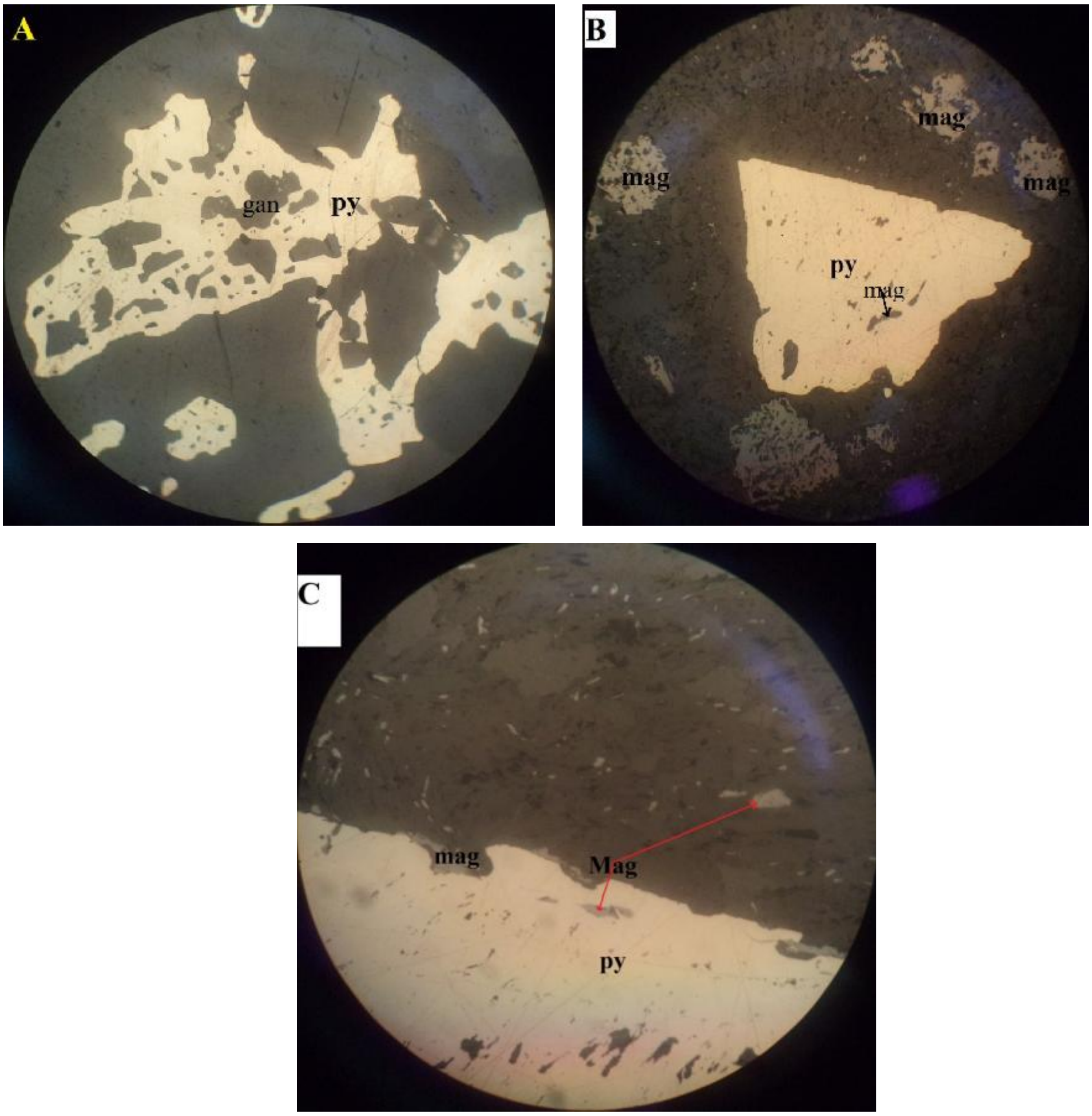

Figure 5.2 Photomicrographs of the various ore minerals to show the distribution and texture of pyrite; and its relationship with other minerals.

A. Photomicrographs of Sample ASDD0002-21, magnification 100 x.
Mineral composition: pyrite 15%, and gangue 85%.
Textural Descriptions / Notes: <u>Spotted and Veinlet texture</u>
Vein of pyrite crystallized across the section following the direction of direction of gangue minerals. Inclusions of gangue minerals enclosed in grains of pyrite give it poikilioblastic texture. Some grains of pyrite lie like spot on the gangue minerals.

B. **Sample ASDD0002-17**, magnification 100 x. displays the distribution and the relationship of magnetite and pyrite.
Mineral composition: magnetite 25%, pyrite 5%, hematite 5% and gangue 65%.
Textural Descriptions. mostly the magnetite have well defined cubic/ idoblastic texture but at times they also found with no defined out line/shape i.e. known as xenoblastic texture. In addition magnetite is also found as inclusion in the idoblastic pyrite. That can suggest magnetite is older than the pyrite; it may also mean that the pyrite is formed at the expense of magnetite by taking the Fe from it.

C. **Sample #ASDD0002-17 (same sample as B) but picture is taken in different view and Magnification (200x).**

5.1.4 Chalcopyrite

This mineral is bright yellow, often found in trace amount with xenoblastic texture. However in few sections significant amount (1-12%) of this mineral also occurs along with the pyrite. The relationship between the pyrite and chalcopyrite is identified in certain polished section (Figure 5.3). In those sections it is observed that the chalcopyrite has either penetrated the boundary of pyrite grains or cross cut the pyrite itself; indicating the chalcopyrite is formed later than pyrites. But rarely the chalcopyrite occurs with pyrite without showing any mineral boundary relationship; that could imply few chalcopyrites were crystallized simultaneously with pyrite.

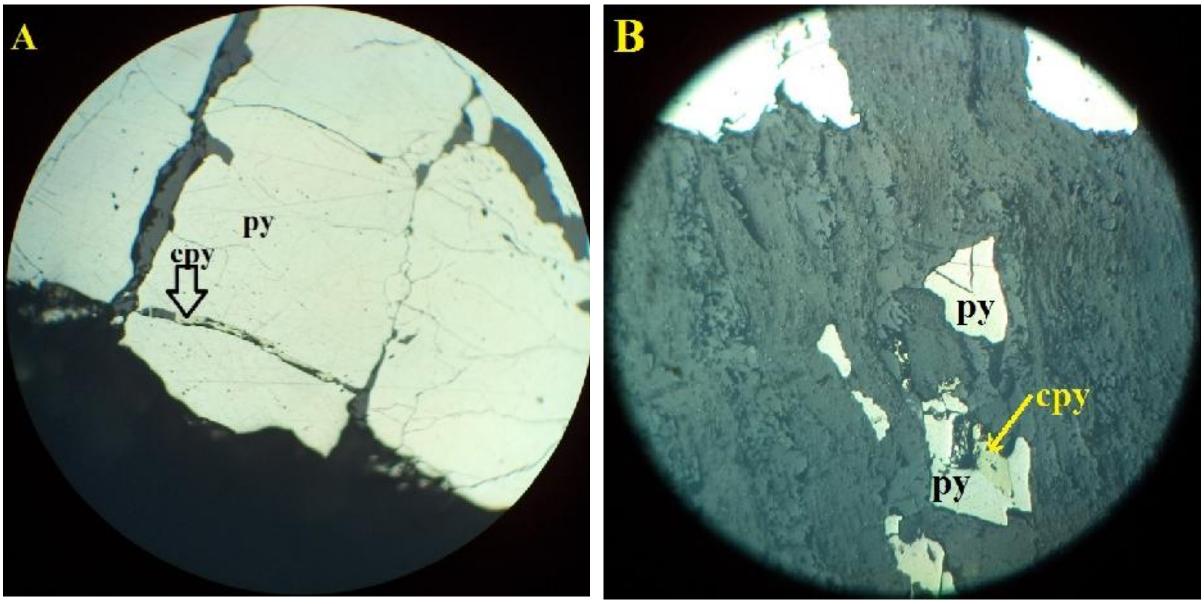

Figure 5.3 Photomicrographs of Sample ASRCD0009-08, to show chalcopyrite and pyrite relationship magnification100 x

A. Photomicrographs of **Sample ASRCD0009-08**, magnification100 x
   Mineral composition: pyrite 65%, Chalcopyrite 1%, gold 3 grains and gangue 34%.
   Textural Descriptions : Veinlet and Massive texture
   Veins of pyrite crystallized across the section following the direction of gangue minerals. Inclusions of three fine grains of gold are seen enclosed on grains of pyrite. Discontinuous and continuous veins of gangue minerals with chalcopyrite are visible cutting the surface of pyrite grains. This implies that the chalcopyrite is formed later than the pyrite, by the rule of cross cutting relationship.

B. Photomicrographs of **Sample # ASRCD0009-09**, magnification100 x.
   Mineral composition: pyrite 30%, Chalcopyrite 3%, and gangue 67%.
   Textural Descriptions / Notes: Veinlet texture
   Pyrite and chalcopyrite crystallized across the section following the direction of gangue minerals. At the lower section of the picture chalcopyrite is clearly seen penetrating into the boundary of pyrite; that indicates the chalcopyrite is relatively younger by the rule of penetration.

5.1.5 Gold

Few grains of gold, up to 6 grains in one polished section are counted under ore microscope. The gold grains are fine and commonly idoblastic, but at times xenoblastic. There is indication that the gold mineralization is associated with phase one pyrite (py1) mineralization, phase two (py2), chalcopyrite and the associated gangue minerals. For instance in, figure 5.4 below, a grain of Au is observed on the pyrite crystal, on other section the Au is found on the gangue that cross cut the Pyrite crystal.

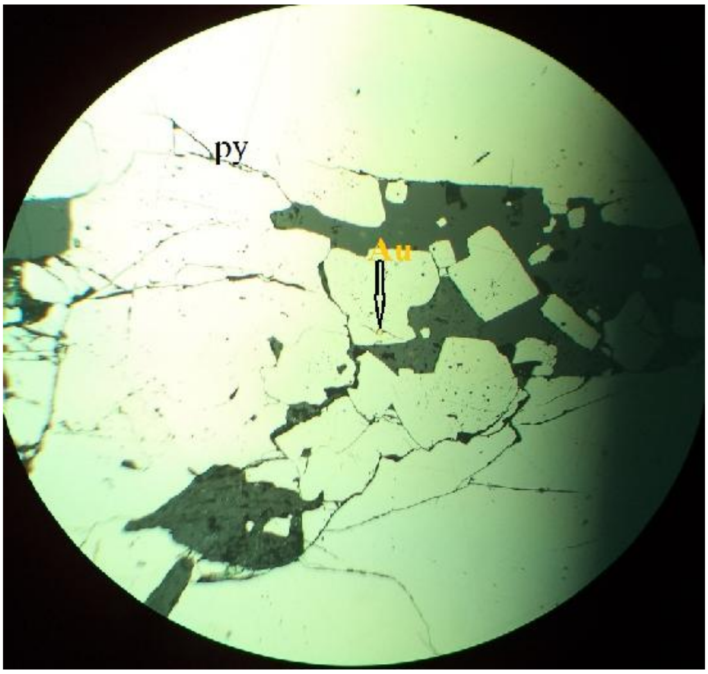

Figure 5.4 Photomicrographs of Sample ASDD0002-18, magnification100 x, to show Au in pyrite (arrow).
Mineral composition: pyrite 35%, Chalcopyrite trace, Au 6 grains and gangue 67%.

Textural Descriptions: Veinlet texture Veins of pyrite crystallized across the section following the direction of gangue minerals. Inclusions of gangue minerals enclosed on grains of pyrite are poikilioblasts. Three fine gold grains growth between grain boundaries of pyrite and gangue minerals, the other three fine lie on grains of pyrite.

5.2 Alteration

Alteration can be defined as a change in texture and mineralogical composition of the country rock due to ascending hydrothermal fluid or descending meteoric water (Evans M, 1987). Generally, alteration can be classified in to two:

1) Primary alteration, which is due to ascending hydrothermal fluids.
2) Supergene (exogenic) alteration which is due to descending (percolating) metoric water interacting with the surrounding rock (Guilbert and Park, 1986; Evans M.1987).

Alteration of the wall rock depends on different factors, such as petrology, chemistry, texture, and physical states, sheard or unsheared character and permeability. For hydrothermal solution the important properties of alteration are: pressure, temperature, ph and Eh. The present day geothermal field is naturally occurring laboratories to show how alteration works in rocks (Evans M., 1987).

Studies of wall rock alterations are important for number of reasons:

1) They increase our understanding concerning the nature of ore forming fluids.
2) They are useful guide in mineral exploration.
3) They are used to determine the age of associated mineralization (Guilbert and Park 1986, Evans M.1987).

Based on integrated investigations of field, microscopic and geochemistry, Ashashire gold mineralization is clearly associated with sulfides in quartz veins and in altered and sheared zones (Figures 3.3 B & C, 5.4 and 5.6). Pyrite is the more dominant sulfide ore mineral than chalcopyrite. The alteration in the area is manifested by the change in color, texture and mineralogy.

Most often, ore bodies of hydrothermal origin results in the alteration of the country rocks that is marked by the change in color, texture and mineralogy or any combination of these (Evans, 1993). Because, hydrothermal solutions contain dissolved ions that are important in ion exchange reactions, and the composition of a particular hydrothermal solution will have an important bearing on the nature of the wall rock alteration it may give rise to. According to him alterations vary from minor color changes to extensive mineralogical transformations and complete recrystallization. Generally speaking, the higher the temperature of deposition of the ore minerals the more intense is the alteration, but it is not necessarily more wide spread. This wall rock alteration, which shows a spatial and usually a close temporal relationship to ore deposits, has variable areal extent; i.e. sometimes being limited to a few centimeters on either side of a vein, at other times forming a thick halo around an ore body.

In agreement with the above Evan's observation the Ashashire mineralization is confined within the altered zone that range from few centimeters to several meters. In other word, the grade of the gold increases in sheared and altered or bleached parts. The alteration is more pronounced in sheared zone of carbonitized chlorite-sericite schist unit and plagioclase-muscovite (sericite)-quartz schist (Figure 5.6 C).

The main alteration assemblages observed in Ashashire is phyllic which is characterized by sericitization. It is a process affecting plagioclase which occurs as phenocryst or as a ground mass, replacing by secondary muscovite. This is formed by hydrolysis of feldspar to form sericite mica with minor association of quartz, chlorite and pyrite. This was seen in the central part of mapped area within carbonitized – chlorite –sericite schist unit.

$3KAlSi_3o_8 + 2H+ (aq) = KAl_3Si_3o_{10} (OH)_2 + 6Sio_2 + 2K+ (aq)$ (Guilbert and Park 1986)

Carbonitization, sulfidation, chloritization , epidotization, silicification, and magnetization are also the styles of alteration existing in the study area. The wall rock alteration brings recrystallization, change in permeability and changes in color such as bleaching (noticed in ASRCD0009, 145-210m and ASDD0002, 131.8-168m, down- hole depth), darkening and various colors.

From drill core logging three main alteration zones are distinguished: an inner colorful fuchsite bearing quartz-calcite-sericite-sulfide zone which displays highest gold content (Figure 5.6 C), an intermediate sericite-chlorite-carbonate-quartz -magnetite zone, and outer zone of actinolite-magnetite-epidote-chlorite alteration. Boundaries among these zones are gradational.

Generally the degree of quartz veining, gold and sulfide enrichment increases from outer towards the inner alteration zones (Figure 5.6).

The major oxide analyses disclose that the alteration at the inner zone/ ore zone (sericitization and carbonitization) is due to the introduction of potassium, calcium, carbon dioxide and water by hydrothermal fluid.

Chlorite rich sediments, possibly reworked mafic volcanic/tuffs, interbedded with fine grained silica rich chert units have been affected by an early phase of actinolite-magnetite-epidote-chlorite alteration, which is best developed in the chlorite sediment (Figure 5.5) due to higher iron content of these sediments. Locally, the more silica rich sediments have thin bands of magnetite that may have replaced chloritic or graphitic layers, and gives the appearance of layered Banded Iron Formation (BIF).

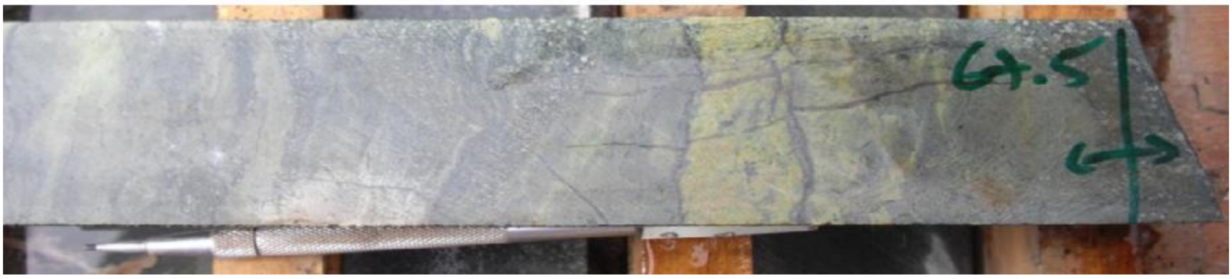

Figure 5.5 Actinolite-magnetite-epidote-chlorite alteration in drill core ASDD0002, 67.5 m depth

The alteration in the intermediate zone/halo is characterized by disseminated, porphyroblastic grains of secondary hydrothermal magnetite. This magnetite is not as unit, but it is part of mineralization and has significance in gold deposition. The elevated magnetite content of the host rock makes them more amenable to wall rock sulphidation reactions and thus quite important for gold deposition implementation.

The chemical reaction by oxidation of ore fluids and wall rock reaction with sulphidation of reactive iron in the host rock brings the alteration of magnetite in to coarse pyrite.

$Au\,(HS)^{-}_{2} + Fe_3O_4 + H^+ = FeS_2 + Au^o + H_2O + \frac{1}{2}\,H_2$ (Guilbert et al., 1986)

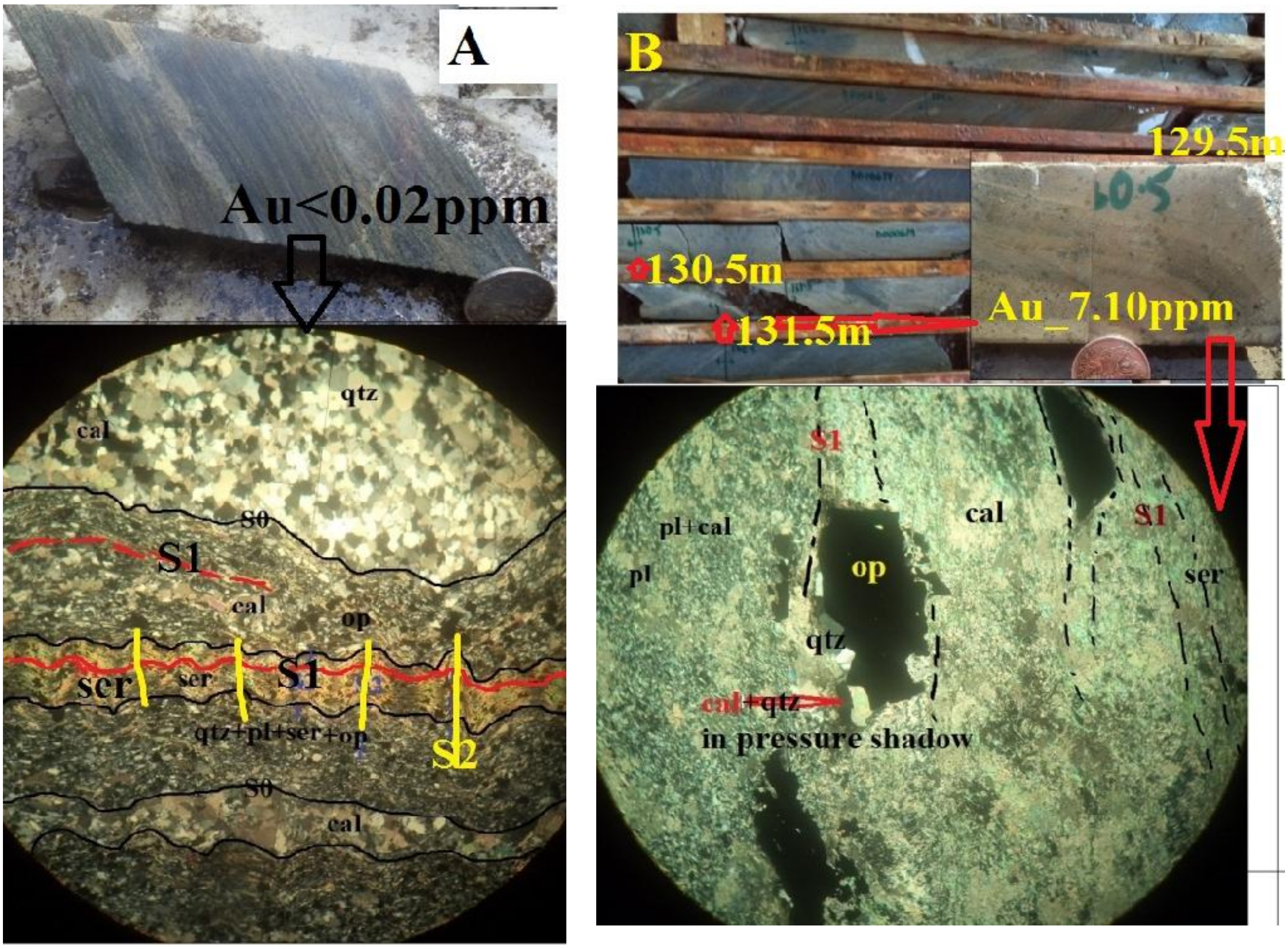
A
Au<0.02ppm
qtz
cal
S0
S1
cal
op
ser
ser
S1
qtz+pl+ser+op
S2
S0
cal
B
129.5m
130.5m
131.5m
Au_7.10ppm
S1
pl+cal
pl
op
cal
S1
ser
qtz
cal+qtz
in pressure shadow

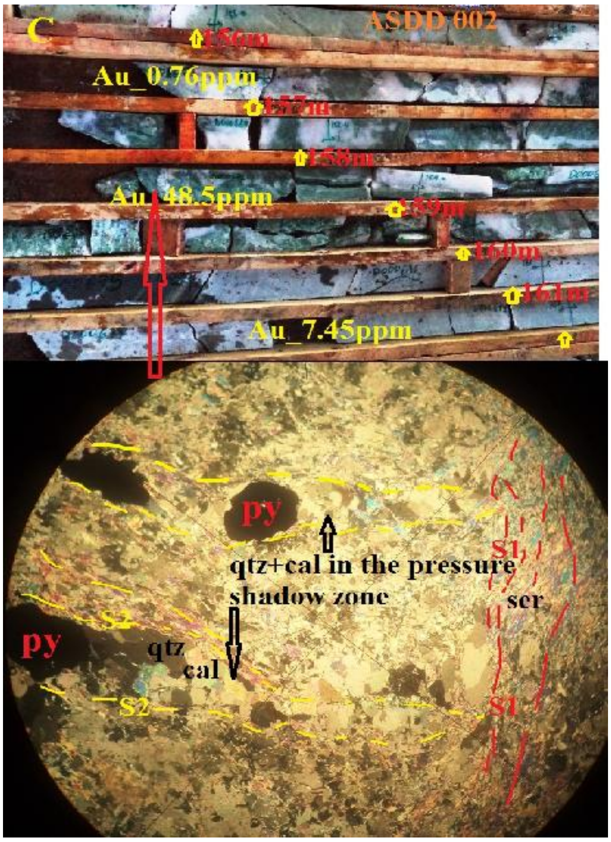

Figure 5.6 Core photos with their respective Au value and Photomicrographs to show how alteration control mineralization i.e Au concentration.

A. unaltered metasediment (calcite-sericite/muscovite-quart schist) core with Au value (<0.02ppm) and Photomicrographs, described in figure 3.2B. sample# ASDD002.

B. **Altered/bleached core with** Au value (7.10ppm at depth of 131.5m) and its reperesentative Photomicrograph from drill hole ASDD0002. The core consits disiminated medium to coarse grained pyrite. Photomicrograph of the sample ASDD002-18A, magnificationn 40x**,**

Mineral content: quartz 30%, muscovite/sericite 25%, calcite 23%, plagioclase 10%, opaque (pyrite) 7%, epidote 3% and chlorite 2%.

Texture and/ or micro structure: the alignment of quartz, calcite and sericite define continuous S1 foliation. The opaque (pyrite) are deformed and align parallel to S1 foliation. Pressure shadow zone, where calcite and quartz crystallized, is formed due to deformation.

Rock name: calcite-sericite-quartz schist.

C. sheared and altered ,mineralize,fuchsite (green mica) bearing core photo with depth and Au value (top) and photomicrograph of sample from the highest Au (48.5ppm) bearing zone(bottom).There are also abundant discoordant and concordant quartz vein lets.

Mineral content: muscovite/sericite 35%, calcite 32%, quartz 20%, , plagioclase 6%, opaque (py) 5% and chlorite 2%.

Texture and/ or micro structure: two phase of deformation is manifested by the alignment of sericite shown by red lines (S1) and S2 (yellow lines) is defined by realignment of sericite, pyrite, crystallized quartz and calcite in the pressure shadow, and it is almost perpendicular to S1 foliation. The pyrite were formed between the two phase of deformation i.e. they overprint S1 foliation implying they crystallized later than S1 but S2 wraps around the pyrite indicating they were formed pre to S2. So the pyrites/mineralization is called intertectonic.

Rock name: quartz-calcite-(muscovite) sericite schist.

5.3 Paragenesis

Integrated analysis, such as field investigations, core samples and ore microscopic studies, helped to understand ore minerals association and their textural relationship among them (Figures 5.1, 5.2, 5.3 & 5.4). Based on these, paragenetic sequence of the ore minerals are attempted to establish in the table below (Table 5.2). Obviously, the silicate minerals that constitute the host lithologies in the study area were formed in the first /early phase. Then, the oxide minerals, magnetite, hematite and ilmenite crystallized in the weakly and/ or unaltered lithologies. However, among the oxides magnetite is formed earlier. The evidence is that hematite is often observed with magnetite either penetrating magnetite grain boundary or replacing it (Figure 5.1). Similarly ilmenite also occurs as a minute grain replacing magnetite. The third stage is the introduction of hydrothermal fluid that caused alteration and the formation of ore/ sulfide minerals and associated gold. Based on the grain boundary relationship between pyrite and chalcopyrite that discussed above, pyrite is the earlier sulfide crystallized (Figure 5.3). However the disseminated magnetite were crystalized earlier than the pyrite by law of inclusions (Figures 5.2 B & C).

Table 5.2 Paragenetic sequence of the minerals constructed based on field and ore microscopic analysis.

Minerals	Sequence of formation (time) early $\longrightarrow$ late		
	Phase I	Phase II	Phase III
Gangue minerals silicate (Chl,act,ep,qtz)			
Oxide minerals			
Magnetite			
Hematite			
Ilmenite			
Wall rock alteration (calcite, sericite & quatz)			
Sulfide minerals and gold			
Pyrite			
chalcopyrite			
Gold			

CHAPTER SIX

6 DISCUSSION

6.1 Possible origin of the gold at Ashashire Prospect

Ashashire is a part of the Precambrian rocks of western Ethiopia that consists of low-grade volcano-sedimentary terrain package of the Arabian-Nubian shield (ANS) bounded both to the east and to the west by the gneissic terrain of the Mozambique Belt (MB) (Asrat et al.2001**,** Fig. 2.3). In other words, the formation of the rocks in the study area is associated to the East African Orogeny that had happened due to the closure of the Mozambique Ocean during the collision of East and West Gondwana that has finally resulted in the formation of Gondwana Supercontinent during the Neoproterozoic era (de Wit and Chewaka 1981; Stern 1994, 2002; Kroner and Stern, 2005) (Figure.2.2). Geochronological data from Precambrian rocks of western Ethiopia also support that the rocks were formed during the Neoproterozoic era.

The Precambrian rocks of western Ethiopia are grouped into five major domain **(**Alemu and Abebe, 2000; Tadesse and Allen, 2005**)**).These are: Daka granitoids, Sirkole volcano-sedimentry sequences, Dengi volcano-sedimentry-plutonic sequences, Tulu Dimitu-Barudu volcano- sedimentry sequences and Didesa gneisses and migmatites **(**Figure 2.4).

According to Tadesse and Allen (2004), trace element analysis using Ti-Zr-Y tectonic discrimination plot confirms the calc-alkaline basaltic character of the Dengi and Sirkole rocks, which constitute the study area, developed in convergent setting; while the Kemashi samples fall in the field of ocean floor basalts representing ocean crust material formed in a spreading environment.

Furthermore, trace element analysis using discrimination diagram (Ti vs. Zr) shows the majority of the rocks of Ashashire area have similar tectonic environment as rocks formed in island arc tholeiites, calc-alkali basalt and mid oceanic ridge basalt (MORB) zone.

Field and thin section study reveal that the study area comprise various units that are deformed, sheared, altered and metamorphosed to green schist facies.

The various litholologies include: granite, plagioclase-muscovite (sericite)-quartz schist, quartz vein, actinolite-quartz-chlorite schist, carbonitized chlorite-sericite-quartz schist and metasediments. The majority of the units have experienced at least two phase of ductile deformations. Phase one deformation (D1) has caused the formation of the pervasive generally N-S trending S1-foliations and associated N to NNE-striking shear zones. Whereas, D2 is manifested by folding of S1 foliation that resulted in recumbent type of folds and associated crenulation lineations.

The mineralized (ore) bodies, carbonitized chlorite-sericite-quartz schist and plagioclase-muscovite (sericite)-quartz schist, are characterized by the presence of sheared, altered/bleached zone (sericitization and carbonatization, green mica fuchsite) and the occurrence of quartz vein.

The Gold mineralization is associated with three-four mineralized zones; namely: hydrothermally bleached zones within the metasediments (with granitic fingering and quartz stringers that contain pyrite disseminations), high grade sheared/brecciated fuchsite-pyrite-chalcopyrite bearing zone, glassy quartz veins and plagioclase-muscovite (sericite)-quartz schist/ sheared granites. Generally, mineralization is confined in ductile shear and altered zones.

Three main alteration zones are distinguished during drill core logging: an inner colorful fuchsite bearing quartz-calcite-sericite-sulfide zone which displays highest gold content (Figure 6.2 C), an intermediate sericite-chlorite-carbonate-quartz -magnetite zone, and outer zone of actinolite-magnetite-epidote-chlorite alteration. Boundaries among these zones are gradational.

The alteration in the intermediate zone/halo is marked by disseminated, porphyroblastic grains of secondary hydrothermal magnetite, which is part of mineralization and has significance in gold deposition. The elevated magnetite content of the host rock makes them more amenable to wall rock sulfidation reactions and thus quite important for gold deposition. The chemical reaction by oxidation of ore fluids and wall rock reaction with sulfidation of reactive iron in the host rock brings the alteration of magnetite in to coarse pyrite.

$Au(HS)^{-}_{2} + Fe_3O_4 + H^+ = FeS_2 + Au^o + H_2O + \frac{1}{2} H_2$ (Guilbert et al., 1986).

Generally the degree of quartz veining, gold and sulfide enrichment increases from outer towards the inner alteration zones. In other word, the grade of the gold dramatically increase in sheared and bleached /sericitized and or carbonitized zones (Figure 5.6).

The major oxide analyses show that the alteration (sericitization and carbonitization) in the inner zone is due to the introduction of potassium, calcium, carbon dioxide and water by hydrothermal fluid.

Hence, the regional geological and structural setting, host rock alteration (silicification, sericitization and carbonatization) and the peripheral propylitic alteration that consist chlorite, epidote, albite and carbonate (calcite), the sulfides (pyrite and chalcopyrite) and gangue (calcite, quartz, and silicates) mineralogy are suggestive for a shear-zone hosted orogenic-gold type deposit at Ashshire (Figure6.1).

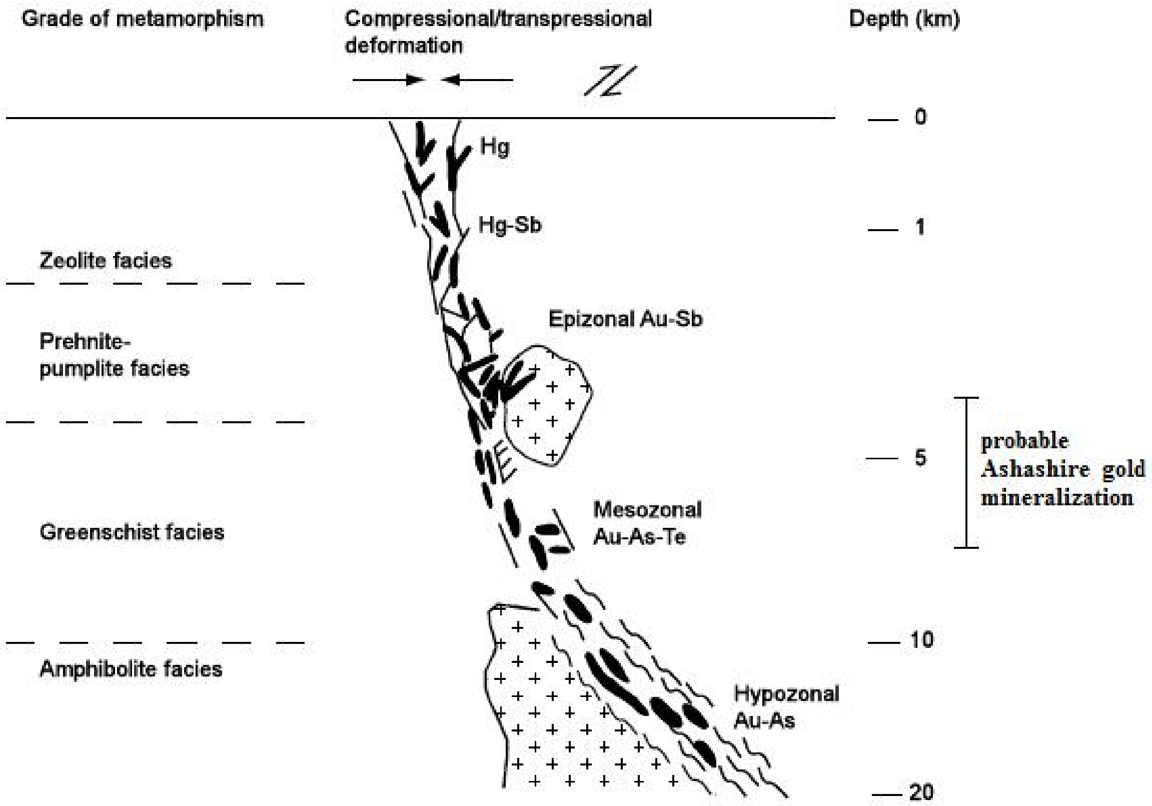

Figure 6.1. Model of orogenic Au deposits representing depth and structural setting (a convergent plate margin) (after Groves et al. 1998; Gebre-Mariam et al. 1995).

CHAPTER SEVEN

7 CONCLUSION AND RECOMMENDATION

7.1 Conclusion

Ashashire area comprises various units that include granite, plagioclase-muscovite (sericite)-quartz schist, quartz vein, actinolite-quartz-chlorite schist, carbonitized chlorite-sericite-quartz schist and metasediments. Based on the presence of critical mineral assemblages such as chlorite, actinolite, epidot, sericite, and muscovite that are identified under microscope, it is interpreted that the rocks in the area have experienced low grade metamorphism that generally belongs to green schist facies.

Field observation and petrography study, reveal that the study area have experienced at least three phase of deformations. Phase one deformation (D1) has caused the formation of the pervasive and the predominant, generally N-S trending S1-foliations and the associated shearing. S1-foliations include schistosity and spaced and continuous cleavages.

On the other hand, D2 has caused the formation of folds and associated crenulation lineations by folding the S1 foliation. However, the east-west trending faults could be related to the later brittle phase of deformation i.e. D3.

Major oxide analysis of fourteen samples using variation/scatter diagram that use K_2O on the X-axis diagram has shown that of K_2O has positive correlation with Al_2O_3 and CaO. These indicate the introduction of potassium, calcium, carbon dioxide and water by hydrothermal fluid that resulted seriticization and carbonitization. In other words, enrichment of muscovite/sericite & calcite are related to the positive correlation of K_2O with Al_2O_3 & CaO. However, K_2O is negatively correlated with MgO, Na_2O and $SiO_{2,}$ which implies that the major elements (Mg, Na and Si) have mobilized while the host rock has been interacted with the mineralizing hydrothermal fluid. Consequently, the altered rocks are depleted in these elements than unaltered rock.

Distribution of trace elements of all samples in chondrite normalized (wood et al., 1979b) spider diagram generally show similar pattern. Particularly the pattern of high field strength elements (HFSE) Zr, Ti & Y shows almost no variation i.e. all samples run parallel to each other; hence, it is interpreted as the rocks are genetically related or they have similar source rock. However the concentration of large ion lithophile elements (LILE) Sr, K, Ba, are higher in altered samples than unaltered samples; that is due to the effect of hydrothermal fluid that has transported these elements. On the other hand the negative anomaly of phosphorous shown by all samples could be associated with the presence of little concentration of apatite in the source rock.

Based on discrimination diagram of Ti vs. Zr, the tectonic environment of majority of the rocks of Ashashire area is similar to island arc tholeiites, calc-alkali basalt and mid oceanic ridge basalt (MORB) zone.

Statistical analysis of AAS data has shown that significant amount of the analyzed data is anomalous in which 49 percent of the samples show Au value above 0.5ppm and only 10% of the data is below the detection limit (0.02 ppm) of the laboratory. These gold anomalous samples are entirely associated to sheared and hydrothermally altered sulfide bearing zone with quartz vein stringers and/ or mineralized quartz vein. Whereas, the samples with assay value less than 0.5ppm are related to weakly and/or unaltered lithologies.

Based on correlation values and the scatter diagrams of Au with the multi elements (with Ag, Cu, Pb, Zn, Ni, Co and Mn), it is concluded that gold has stronger positive association with silver (Ag) than any other metals. That implies the fluid that transported gold is also enriched with the silver (Ag).

The ore bodies, carbonitized chlorite-sericite-quartz schist and plagioclase-muscovite (sericite)-quartz schist are characterized by the presence of sheared, altered/bleached zone and the occurrence of quartz veins. Generally, the grade of the gold is controlled by alteration and shear zone.

The paragenesis or sequence of formation of ore minerals such as pyrite chalcopyrite, magnetite, hematite, ilmenite and gold is constructed based on field observation and textural relationship among them. Accordingly the silicate minerals/ the gangue that constitute the host rock are formed in the earliest phase then, magnetite hematite, ilmenite, pyrite, chalcopyrite and gold are crystallized respectively.

Based on the regional geological and structural setting, host rock alteration (silicification, sericitization and carbonatization) and the peripheral propylitic alteration that consist chlorite, epidote, albite and carbonate (calcite), the sulfides (pyrite and chalcopyrite) and gangue (calcite, quartz, and silicates) mineralogy, it is interpreted that the deposit type at Ashashire could be a shear-zone hosted orogenic-gold deposit.

7.2 Recommendations

- Integrated structural and geophysical study is highly recommended to understand the role of different phase of deformation and associated structures in controlling the mineralization in the Ashashire Prospect.
- To know the source of mineralizing fluid it is also recommended to conduct different type of study such as fluid inclusion analysis.
- Ashashire Prospect is not recommended for base metals (Cu, Pb, & Zn) exploration.

REFERENCES

Abraham, A. (1989). Tectonic history of the Pan-African low-grade belt of western Ethiopia. Note 305, Ethiopian Institute of Geological Surveys, Addis Ababa, 15 pp.

Ahmed M.(1982). Report on Kurmuk-Geisan Integrated Mineral Exploration Project. Ethiopian Institute of Geological Survey. Note Nr.208.

Alemu, T. and Abebe, T. (2000). Geology of the Gimbi area. Unpublished technical report, Geological Survey of Ethiopia, Addis Ababa, Ethiopia.

Alene, M., Ruffini,R.,and Sacchi, R., 2000. Geochemistry and geotectonic setting of Neoproterozoic rocks from northern Ethiopia (Arabian-Nubian Shield). Gondwana Research 3, 333-347.

Allen, A.R., and Tadesse, G.(2003). Geological setting and tectonic subdivision of the Neoproterozoic Orogenic Belt of Tuludimtu,western Ethiopia. Journal of African Earth Sciences 36, 329–343.

Asrat, A., Barbey, P., and Gleizes, G. (2001). The Precambrian Geology of Ethiopia: a review. Africa Geoscience Review, 8, 271-288.

Ayalew, T., Bell, K., Moore, J.M., and Parrish, R.R.(1990). U-Pb and Rb-Sr geochronology of the Western Ethiopian Shield. Geological Society America Bulletin 102, 1309-1316.

Braathen,A.,Grenne,T.,Selassie,M.G.,Worku,T.(2001).Juxtaposition of Neoproterozoic units along the Baruda-Tulu Dimitu shear-belt in the Eastern African Orogen of western Ethiopia. Precambrian Research, **107**: 215-234 Bulletin Geophysics. Obs., Addis Ababa University 15, 27-43.

Cawood, P.A., Kroner, A., Collins, W.J., Kusky, T.M., Mooney, W.D., Windley, B.F.(2009). Accretionary Orogens through Earth History. Geological Society of London, Special Publication 2009, vol. 318: 1–36.

Chewaka, S., and De Wit, M.J.(1981). Plate tectonics and metallogenesis: some guidelines to Ethiopian Mineral Deposits, Ethiopian Institute of Geological Surveys, Bulletin 2, pp129.

De Wit, M.J., and Chewaka, S. (1981). Plate tectonic evolution of Ethiopia and the origin of its mineral deposits: an overview. In: Chewaka, S., and de Wit, M.J. (eds.), Plate tectonics and metallogenesis: some guidelines to Ethiopian Mineral Deposits, Ethiopian Institute of Geological Surveys Bulletin 2, 115-129.

Evans, A.M. (1993), An introduction to ore geology and industrial minerals, 3rd ed. Blackwell Scientific Publications, USA, pp 134-136.

Fontana G.,(1954) Benishangul Gold Placer. Ethiopian Institute of Geological Survey. Unpublished report.

Gebremariam, M., Hagemann, S.G., and Groves, D.I., 1995. A classification scheme for epigenetic Archean load –gold deposits. Mineral deposita, 30:408-410.

Golden Star Resources Limited Ethiopia:Dul Exploration Annual Report, May 31, 1996. Report no. 041-351-43.

Gray, D. R.,Foster,D. A., Meert, J. G., Goscombe, B. D., Armstrong,R., Truow, R. A. J. & Passchier, C. W. (2008). A Damaran Perspective on the Assembly of Southwestern Gondwana. Geological Society,London, Special Publications, 294: 257–278.

Groves, D.I., Goldfarb, R.J., Gebremariam, M., Hagemann, S.G., and Robert, F., 1998. Orogenic gold deposits: A proposed classification in the contexet of their crustal distribution and relation to other gold deposit types. Ore Geology Reviews, 13: 7-27

Guilbert, J.M., and Park, Jr., F.P.(1986). The geology of ore deposits. W.H. Freeman and Company, USA, 985 pages.

Hess, R. (1932). The province of Benishangul in west Abyssinia as a gold producer. Note nr.151

Huntington Geology and Geophysics Limited.(1969). Mineral survey in two selected areas in Ethiopia, Photogeological survey, Vol 1, pt 1&2. Ministry of Mines & Energy, Addis Ababa, Ethiopia.

Jelenc, D. (1966). Mineral occurrences of Ethiopia. Ministry of Mines, Addis Ababa.

Jembere, M. (1984). Geochemical exploration of Shingu-Shide, Belaute-Dul Gule &Edemgash area:Wellega Province,810-351-07.

Jembere M. (1995). Dul primary and regolith related gold deposit, Exploration and Evaluation.EIGS, Addis Ababa.

Johnson, P.R., Abdelsalam, M.G., Stern, R.J. (2003). The Bi'r Umq-Nakasib suture zone in the Arabian–Nubian Shield: a key to understanding crustal growth in the East African Orogen. Gondwana Research, 6 :523–530.

Johnson, T.E., Ayalew, T., Mogessie, A., Kruger, F.J., Poujol, M.(2004). Constraints on the tectonometamorphic evolution of the western Ethiopian Shield. Precambrian Research. 133, 305–327.

Johnson, P.R., Andresen, A., Collins, A.S., Fowler, A.R., Fritz, H., Ghebreab, W., Kusky, T. and Stern, R.J.(2011).Late Cryogenian–Ediacaran history of the Arabian–Nubian Shield: A review of depositional, plutonic, structural, and tectonic events in the closing stages of the northern East African Orogen, Journal of African Earth Sciences. **61**: 167–232

Kazmin, V., 1971. Precambrian of Ethiopia. Nature 230, 176-177.

Kazmin, V. (1975). The Precambrian of Ethiopia and some aspects of the geology of the Mozambique Belt.

Kazmin, V., Shiferaw, A., and Balcha, T.(1978). The Ethiopian basement and possible manner of evolution, Geologische Rundschau **67**:531-546.

Kebede, T., Koeberl, C. (2003). Petrogenesis of A-type granitoids from the Wallagga area, western Ethiopia: constraints from mineralogy, bulk-rock chemistry, Nd and Sr isotopic compositions. Precambrian Research, **121:**1–24.

Kroner, A., and Stern, R.J.(2005).Pan- African Orogeny. Encyclopedia of Geology, v. 1. Elsevier, Amsterdam, www.utdallas.edu/~rjstern/pdfs/PanAfricanOrogeny.pdf .viewed 18 Dec 2013.

Meert, J. G. & Lieberman, B. S. (2008). The Neoproterozoic Assembly of Gondwana and its relationship to the Ediacaran–Cambrian radiation. Gondwana Research, 14:5–21.

Metal Mining Agency of Japan, (1974). Report on Geological Survey of Western Wellega.

Pearce, J.A., and Cann, J.R. (1973). Tectonic setting of basic volcanic rocks determined using trace element analyses. Earth Planet. Scientfic Letter. 9:290–300.

Rollinson, H.R. (1993). Using Geochemical Data; Evaluation, Presentation, Interpretation. Longman Group Ltd., London, pp. 343.

Stern, R.J. (1994). Arc assembly and continental collision in the Neoproterozoic East African Orogen: implications for consolidation of Gondwana land. Annual Reviews Earth Planetary Sciences **22**: 319-351.

Stern, R.J.,(2002).Crustal evolution in the East African Orogen: a neodymium isotopic perspective.Journal of African Earth Sciences, **34**:109–117.

Stern, R.J., and Johnson, P.R. (2010). Continental lithosphere of the Arabian Plate: a geologic, petrologic, and geophysical synthesis. Earth-Science Reviews **101**:29–67.

Tadesse, T., Suzuki, K., Hoshino, M., 1997. Chemical Th–U total Pb isochron age of zircon from the Mareb Granite in northern Ethiopia. J. Earth Planet. Sci. Negoya Univ. 44, 21–27.

Tadesse, T., Hoshino, M., and Sawada, Y., 1999. Geochemistry of low-grade metavolcanic rocks from the Pan African of the Axum area, northern Ethiopia. Precambrian Research,99, 101-124.

Tadesse, T., Hoshino, M., Suzuki, K., and Iisumi, S., 2000. Sm-Nd, Rb-Sr, and Th-U-Pb zircon ages of syn- and post-tectonic granitoids from the Axum area of northern Ethiopia. Journal of African Earth Sciences 30, 313-327.

Tadesse, G., and Allen, A.R. (2004). Geochemistry of metavolcanics from the Neoproterozoic Tuludimtu Orogenic Belt, western Ethiopia. Journal of .African. Earth Sciences, **39**:177–185.

Tadesse, G., and Allen, A.R. (2005). Geology and geochemistry of the Neoproterozoic Tuludimtu Ophiolite Belt, western Ethiopia. Journal of African Earth Sciences, 4:192–211.

Tadesse, S. (2009). Mineral Resources Potential of Ethiopia , Addis Ababa University printing press, Addis Ababa, Ethiopia.

UNDP,1972. Mineral survey in two selected areas (Sidamo & Wellega).

Usoni, L. (1952). Mineral Occurrence Map of Ethiopia. Ethiopian Institute of Geological Surveys Bulletin. Unpublished report.

Wood D.A., Tarney J., Varet J., Saunders A.D., Bougault H., Joron J.L., Treuil M. and Cann J.R. (1979b). Geochemistry of basalts drilled in the North Atlantic by IPOD Leg 49: Implications for mantle hetrogenity. Earth Planetary Science Letter, **42**:77-97.

Yibas, B., 2000. The Precambrian geology, tectonic evolution, and controls of gold mineralisations in southern Ethiopia. Ph.D. Thesis (unpublished), University of the Witwatersrand, Johannesburg, South Africa, 448 pp.

Yibas, B., Reimold, W.U., Anhaeusser, C.R., (2000a). The geology of the Precambrian of southern Ethiopia: I—the tectono-stratigraphic record. Information Circular 344, Economic Geology Research Institute, University of the Witwatersrand, Johannesburg, pp 21.

Yibas, B., Reimold, W.U., Armstrong, R., Koeberl, C., Anhaeusser, C.R., Phillips, D.(2002). The tectonostratigraphy, granitoid geochronology and geological evolution of the Precambrian of southern Ethiopia. Journal of African Earth Sciences, **34**:57–84.

Zubaer A. (1986). The Geology of Kurmuk-Asosa sheet. Department of Regional Mapping. Unpublished report.

Annexes

Annex 1: Geochemical AAS analysis data

CERTIFICATE OF ANALYSIS

LAB JOB NO. EAL-13A0147

CLIENT NAME:ABEBE BEDESSA

ADDRESS: Addis Ababa

ATT:

TEL.:

INVOICE: BEC/263/13

CLIENT REF.: ABD-062

NO. SAMPLES: 40

SAMPLE TYPE: Core

SAMPLES RECEIVED: 10/12/2013

ANALYSIS INSTRUCTIONS RECEIVED 10/12/2013

DATE OF REPORT: 24/12/2013

STATUS OF REPORT: Final

ANALYSIS COMPLETE: 23/12/2013

Management Signator

Daniel Admasu QA/QC Manager

Technical Signatories

Yirgaalem W/gebriel, Laboratory Manager

Dawit G/michael, Analysis Supervisor

This report relates specifically to the sample(s) tested in so far as that the sample(s) is truly representative of the sample source as supplied.

Notes/Comments:

No	Sample idents	Au	Ag	Cu	Co	Pb	Ni	Zn
1	ASRC 0002-01	0.66	0.7	78	11	1	19	32
2	ASRC 0002-02	0.03	<0.2	27	8	<1	15	32
3	ASRC 0002-03	1.11	0.9	19	20	<1	11	63
4	ASRC 0002-04	0.50	0.8	94	15	1	31	55
5	ASRC 0002-05	0.09	1.0	70	34	<1	35	75
6	ASRC 0002-06	0.06	0.7	31	19	<1	44	47
7	ASRC 0002-07	<0.02	0.7	39	21	<1	86	52
8	ASRC 0002-08	0.02	0.8	43	22	<1	50	49
9	ASRC 0002-09	0.12	1.0	80	29	<1	36	57
10	ASRC 0002-10	0.03	1.1	120	38	<1	24	83
11	ASRC 0003-11	1.50	1.1	94	28	<1	27	58
12	ASRC 0003-12	3.26	1.3	64	30	<1	26	74
13	ASRC 0003-13	0.38	1.1	30	31	<1	25	79
14	ASRC 0003-14	1.90	1.1	107	35	<1	29	78
15	ASRC 0003-15	0.15	1.0	97	37	<1	30	63
16	ASRC 0003-16	0.25	1.0	104	33	<1	25	67
17	ASRC 0003-17	5.23	1.2	270	40	<1	29	73

18	ASRC 0003-18	0.42	1.1	79	34	<1	24	60
19	ASRC 0003-19	0.27	0.6	11	16	<1	10	52
20	ASRC 0003-20	0.62	0.8	38	21	<1	5	61
21	ASDD 0002-07	1.91	1.0	80	35	<1	33	73
22	ASDD 0002-13	<0.02	1.0	33	26	<1	4	50
23	ASDD 0002-18	7.10	1.1	18	11	1	9	34
24	ASDD 0002-19	1.64	1.5	180	35	2	41	90
25	ASDD 0002-20	0.76	0.4	<1	11	<1	17	20
26	ASDD 0002-22	48.5	4.9	55	44	2	266	65
No	**Sample idents**	**Au**	**Ag**	**Cu**	**Co**	**Pb**	**Ni**	**Zn**
27	ASDD 0002-23	7.45	7.4	3400	42	1	113	77
28	ASDD 0002-24	0.32	0.9	8	29	<1	29	51
29	ASDD 0002-25	<0.02	0.8	42	23	<1	14	39
30	ASDD 0005-31	0.05	0.8	47	23	<1	20	67
31	ASDD 0005-33	<0.02	<0.2	43	5	2	2	10
32	ASDD 0005-36	0.03	<0.2	9	5	<1	3	46
33	ASDD 0005-38	<0.02	<0.2	11	4	<1	3	13
34	ASRCD 0009-03	0.42	0.9	82	31	<1	31	58
35	ASRCD 0009-06	16.00	2.2	74	28	1	22	74
36	ASRCD 0009-08	8.46	1.6	25	49	<1	29	46
37	ASRCD 0009-09	0.50	0.7	35	16	<1	15	44
38	ASRCD 0009-10	1.08	0.4	6	10	1	25	30
39	ASRCD 0009-11	<0.02	1.0	38	26	<1	11	52
40	Way Paint-327	4.25	0.7	26	2	<1	3	2
	UNITS	Ppm	ppm	ppm	ppm	ppm	ppm	ppm
	DET.LIM	0.2	0.2	1	1	1	1	1
	METHOD CODE	AA74D2	AA74D2	AA74D2	AA74D2	AA74D2	AA74D2	AA74D2
	PREPARATION CODE	PG210	PG210	PG210	PG210	PG210	PG210	PG210

Annex 2: XRF analysis data

Geochemical Laboratory XRF Analysis Report Format: Form GD0008

File ID:-	**1912Pvt**	**Customer Type:**	**pvt**
Originator:-ABEBE BEDASSAI		**Date Submitted**	**18-09-2013**
Sample type:- ROCK		**Date Completed**	**MAR-14-2014**
Preparation: -200mesh		**NUMBER OF SAMPLES**	**14**
Analytical Method: Xrf with Pressed pellets			

		Element in (%)										
Lab. No.	**Field No.**	**SiO_2**	**Al_2O_3**	**Fe_2O_3**	**CaO**	**MgO**	**Na_2O**	**K_2O**	**TiO_2**	**MnO**	**P_2O_5**	**LOI**
1912-14	ASDD0002-18	80.39	5.30	3.37	3.21	2.44	0.37	0.52	0.18	0.07	0.09	3.96
1913-14	ASDD0002-19	34.00	17.57	8.49	11.95	7.56	3.85	2.16	1.36	0.23	0.03	12.53
1914-14	ASDD0002-22	48.95	12.65	7.24	9.65	7.19	1.25	2.73	0.22	0.14	0.02	9.59
1915-14	ASDD0002-23	38.96	14.72	8.65	10.88	8.11	2.07	3.56	0.55	0.19	0.03	11.75
1916-14	ASRCD0009-0	38.38	17.83	8.82	9.33	6.43	3.44	2.68	0.92	0.20	0.04	11.66
1917-14	ASRCD0009-0	48.54	14.17	11.67	6.09	4.14	2.00	2.55	0.99	0.12	0.03	9.51
1918-14	ASRCD0009-0	65.65	12.60	4.25	4.04	2.79	1.07	2.31	0.72	0.09	0.04	5.61
1919-14	wat-point-323	38.88	4.27	5.93	0.46	37.26	0.39	0.06	0.03	0.14	0.01	0.00
1920-14	ASDD0005-34	46.01	14.29	12.58	6.50	8.69	4.00	0.20	1.08	0.54	0.11	5.74
1920-14D	ASDD0002-1	45.76	14.28	12.53	6.59	8.61	3.95	0.20	1.11	0.53	0.11	6.09
1921-14	ASDD0002-29	51.94	13.64	8.45	6.53	9.84	4.13	1.69	0.68	0.14	0.05	2.60
1922-14	ASDD0005-34	66.00	13.68	4.73	3.05	1.77	5.14	1.86	0.45	0.25	0.07	2.86
1923-14	ASDD0005-39	70.60	12.46	4.75	1.43	1.82	6.77	0.18	0.46	0.06	0.07	1.24
1924-14	ASDD0005-40	45.07	15.32	9.89	1.02	17.33	1.07	1.68	0.46	0.57	0.08	7.10
1925-11	ASDD0005-44	52.66	12.01	10.14	5.24	10.12	5.21	0.88	0.27	0.18	0.04	3.03

The results indicated above are result of the sample that submitted to the laboratory

Analysts	Checked By	Quality Control	Date Reported
Dawit T.			**Mar-14-2014**
Almaz E.			

Lab. No.	**Field No.**	Sr	Sc	Y	Ba	Zr	Nb	Mo	Pb	Zn	Co	Cu
1912-14	ASDD0002-18	163	10	21	386	157	<5	<3		34	22	37
1913-14	ASDD0002-19	811	15	22	330	134	<5	<3	29	92	21	144
1914-14	ASDD0002-22	386	13	18	336	44	<5	<3	30	77	25	45
1915-14	ASDD0002-23	445	16	19	344	57	<5	<3	30	80	27	1984
1916-14	ASRCD0009-0	461	15	21	337	91	<5	<3	29	77	16	65
1917-14	ASRCD0009-0	263	13	18	274	60	<5	<3	26	41	37	28
1918-14	ASRCD0009-0	381	12	24	459	78	<5	<3	37	53	11	38
1919-14	wat-point-323	2	12	23	439	2	<5	<3	62	17	111	19
1920-14	ASDD0005-34	110	15	20	281	66	<5	<3	28	65	50	85
1920-14D	ASDD0002-1	110	15	20	282	67	<5	<3	28	66	50	85
1921-14	ASDD0002-29	204	15	21	393	52	6	<3	31	54	37	55
1922-14	ASDD0005-34	69	11	31	436	148	<5	<3	39	69	9	22
1923-14	ASDD0005-39	78	11	30	453	151	14	<3	41	89	19	18
1924-14	ASDD0005-40	30	15	20	437	39	<5	<3	35	1212	16	133
1925-11	ASDD0005-44	40	16	19	347	39	6	<3	32	68	36	47

Annex 3: drill core logging data

Drill-hole ASDD0002,

Depth interval (M)	Lithology and chip core samples
0.0-2.02	Saprolite
2.02-2.32	Quartz vein
2.32-4.73	Weathered mafic intrusive
4.73-8.59	Unknown altered
8.59-22.39	Medium massive intrusive with epidote enrichment(sample ASDD0002-01 at 20m)
22.39-28.22	Metasediment with medium-coarse phenocryst of of feldspar (sample ASDD0002-02 at 26.5m)
28.22-28.94	Foliated mafic intrusive with high magnetite content and chlorite (sample ASDD0002-03 at 28.3m)
28.94-31.68	Medium mafic intrusive with carbonate (sample ASDD0002-04 at 31.2)
31.68-39.15	Foliated metasediment package with high content of magnetite
39.15-41.47	Medium mafic intrusive with phenocryst of feldspar
41.47-58.63	Weakly to moderately silicified metasediment including massive intrusive (sample ASDD0002-05 , 06, and 07 at 51m , 53m and 55.5m respectively)
58.63-62.24	Medium mafic intrusive
62.24-69.09	Metasediment rich in chlorite and phenocryst of feldspar (sample ASDD0002-08 at 65m)
69.09-77.62	Mafic intrusive rich in carbonate, partly silicified (sample ASDD0002-09 and 10 at 72m and 73.5m respectively)
77.62-85-41	Chlorite schist quartz feldspar and carbonate (sample ASDD0002-11 at 82m respectively)
85.41-89.3	Graphite schist chlorite silicified metasediment (sample ASDD0002-12 at 87.5)
89.3-99.65	Chlorite- quartz feldspar with magnetite (sample ASDD0002-13 at 99m)
99.65-106	Metasediment package rich in phenocryst of feldspar (sample ASDD0002-14 at 105m)
106-107.4	Foliated metasediment
107.4-113.72	moderate sililicified mafic intrusive with 24 cm quartz vein at 109.58 m. (sample ASDD0002-15 at 108m)
113.72-114.54	Felsic intrusive weakly silicified (sample ASDD0002-16 at 114m)
114.54-115.94	Medium mafic intrusive
115.94-118.5	Chlorite-quartz schist rock
118.5-121.5	Highly foliated and moderately silicified including 30cm quartz vein
121.5-125.13	Weakly silicified medium grained metasediments
125.13-125.61	Weakly silicified massive intrusive (sample ASDD0002-17 at 125.2m)
125-61-138.58	Moderately to strongly silicified mafic intrusive (sample ASDD0002-18 and 19 at 131.8m and 149.3m respectively) brecciated
138.58-156.83	Felsic intrusive interbeded with several mafic intrusive (sample ASDD0002-20 at 156.7m)
156.58-160.13	Quartz vein with malachite and tourmaline , breccia load (sample ASDD0002-21at 157.8m)
160.13-168.27	Chlorite-quartz-feldspar with fine-coarse grained massive undifferentiated (sample ASDD0002-22, 23,24 and 25at 158.7m , 161.5m, 165.3m, and 167.5m

	respectively)
168.27-187.64	Quartz-chlorite-feldspar schist (sample ASDD0002-26 at 187.5m)
187.64-190.25	Mafic intrusive weak-strongly silicified
190.25-201.63	Mafic schist strongly silicified (sample ASDD0002-27 at 192m)
201.63-231.15	Mafic schist to mafic intrusive, weak –strongly silicified (sample ASDD0002-28 and 29 at 223.5 and 241.5m)

Drill-hole ASRCD0009,

0.0-70 m	Rotary circulation (RC) powder samples
70-72.09	Chloritized and epidotized BIF
72.09-75.94	Epidotized chlorite schist
75.94-82.44	Chloritized BIF with feldspar phenocryst (sample ASRCD0009-01 at 78.35m)
82.44-94.18	Epidotized BIF with chert
94.18-96.52	Chloritized BIF with feldspar phenocryst
96.52-101.87	Chlorite schist with disseminated magnetite and feldspar phenocryst
101.87-115.26	Magnetiferous bleached chlorite sericite schist (sample ASRCD0009-02 at 107.9m)
115.26-119.87	Chlorite sericite with deformed magnetite
119.87-129.5	Magnetiferous bleached chlorite sericte schist (sample ASRCD0009-03 at 124.5m)
129.5-133.96	Chloritized BIF with secondary magnetite phenocrysts
133.96-143.02	Strongly epidotized chlorite schist with disseminated coarse magnetite Clasts following foliation plane (sample ASRCD0009-04 at 135.7m)
143.02-145.05	Magnetiferous chlorite sericite schist
145.05-151.6	Magnetiferous bleached quartz-chlorite-sericite schist (sample ASRCD-05 at 147.9m)
151.6-154.75	Quartz-sericite schist
154.75-155.83	Chert with interbeds of chlorite sericite schist
155.83-162.53	Magnetiferous bleached quartz –sericite-chlorite schist (sample ASRCD0009-06 at 162.1m)
162.53-164.94	Brecciated and bleach sericite-chlorite sericite schist with quartz veining (sample ASRCD0009-08 at 164.7)
164.94-178.75	Strongly bleached magnetiferous chlorite schist (sample ASRCD0009-07 at 178.3m)
178.75-188.66	Bleached magnetiferous chlorite-sericite schist
188.66-194.83	Sericite schist banded at plaaces and feldspar phenocryst
194.83-195.38	Sheard granite
195.38-198.19	Quartz sericite schist with bands of dark grey minerals
198.19-203.44	Sericite-chlorite schist with disseminated magnetite
203.44-207.66	Quartz-sericite schist
207.66-210.55	bleached(albitized) sericite-chlorite schist with 0.6m sheard granite
210.55-222.53	Highly sheard granite with quartz vein and brecciated zone filled with fuchsite and tourmaline (sample ASRCD0009-09 and 10 at 210.8m and at 220.4 m respectively)
222.53-229.08	Magnetiferous, moderately bleached quartz chlorite schist
229.08-234.41	Chlorite serite schist with bands of BIF and carbonate
234.41-237.75	Chloritized BIF
237.75-238.16	Mafic to intermediate intrusive
238.16-240.55	Sheard chloritized BIF (sample ASRCD0009-11 at 238.15m)
240.55-241.52	Chloritized BIF with phenocryst of feldspar
241.52-244.52	Bands of chlorit-sericite, BIF chert with phenocryst of feldspar
244.52-248.5	Bands of chlorit-sericte schist, BIF and chert,and phorphyritic intrusive at 248.14 m